Wood Science and Technology (2023) 57:989–1037
https://doi.org/10.1007/s00226-023-01484-4

REVIEW

Functional materials based on wood, carbon nanotubes, and graphene: manufacturing, applications, and green perspectives

Damian Łukawski[1] · Patrycja Hochmańska-Kaniewska[2] · Dominika Janiszewska-Latterini[2] · Agnieszka Lekawa-Raus[3]

Received: 17 April 2023 / Accepted: 25 July 2023 / Published online: 12 August 2023

Abstract

Driven by the quest for greener and more sustainable materials, the presented review analyzes recent studies in which wood and wood-based materials were combined with carbon nanomaterials in the form of carbon nanotubes and graphene. The analysis shows a close kinship between these two carbon-based materials. The first studies have shown that wood may be directly transformed into sp^2-bonded carbons, i.e., form graphene-like structures. Further, it has been demonstrated that both carbon nanotubes and graphene can be used to coat or infiltrate wood and processed wood-based materials such as flexible wood sponges or biochars. Thanks to the unique electrical, mechanical, thermal, and wetting properties of graphene and carbon nanotubes, their wood-based nanocomposites were shown to have many potential applications in green electronics area or as nanodevices. Finally, a new range of studies in the area of wood composites showed that carbon nanomaterials integrated into wood-based boards could improve the properties of the former ones. The presented review shows that this emerging area of research on wood-based materials, graphene, and carbon nanotubes is highly promising and interesting in the context of new applications and future perspectives for sustainable development.

✉ Agnieszka Lekawa-Raus
agnieszka.raus@pw.edu.pl

[1] Institute of Physics, Faculty of Materials Engineering and Technical Physics, Poznan University of Technology, Piotrowo 3, 61-139 Poznan, Poland

[2] Center of Wood Technology, Łukasiewicz Research Network—Poznań Institute of Technology, ul. Winiarska 1, 60-654 Poznan, Poland

[3] Centre for Advanced Materials and Technologies, CEZAMAT, Warsaw University of Technology, ul. Poleczki 19, 02-822 Warsaw, Poland

Introduction

The urgent need for materials that have a low impact on the environment, both during the manufacture, use, and at the end of their lifecycle, drives the attention of scientists toward natural materials such as wood. Wood is a highly abundant and versatile material that has been serving humans for thousands of years as the first source of energy, tools, the basis of construction, thermal insulation, and furniture. Although it has been replaced in many areas by steel, concrete or synthetic polymers, wood and its derivatives are still broadly applied in the construction of buildings, interior furnishings, and outdoor structures. This is mainly due to its visual qualities, good mechanical performance, insulating properties, and relative lightweight.

In botanical terms, wood is the tissue of trees and other plants. Up to this point, trees were the primary source of wood; however, today's technology also uses the wood of shrubs, and even the fibers of annual and perennial plants, for example, bamboo plants. Wood, as a material, has a complex structure and anisotropic properties. It is composed of fibers oriented parallel to the tree trunk and ray cells running perpendicular to the fibers. This natural tissue is responsible for strengthening and nutrient conducting. To understand the complex nature of this material, the macroscopic, microscopic, and chemical structure of wood should be studied (Ross 2021). Natural wood is a highly porous structure made of elongated cells. The anatomy of wood differs between the groups of coniferous (softwoods) and deciduous (hardwoods) species. Softwoods (like pine wood) are composed predominantly of tracheids, and hardwoods (like oak wood) are mainly made of fibers and vessels. Tracheids and vessels are the principal water-conducting cells, while the main function of fibers is to provide mechanical support (Wilson and White 1986; Richter 2015). The cell walls are made of cellulose surrounded by a matrix of hemicellulose and lignin. Those three main components constitute 90–95% of the weight of absolutely dry wood and have different features that work together to impart the physical integrity of the cell wall. The remaining 5–10% are extractives containing, inter alia, essential oils, resins, waxes, fats, tannins, and alkaloids. Although extractives are not structural components, they are responsible for the odor, color, and decay resistance, they also affect painting and glue adhesion (Sjöström 1993; Rowell 2021).

Wood structure's chemical and anatomical details impart wood properties such as hardness, mechanical strength, low density, high porosity, thermal insulation, hygroscopicity, etc. Density, as one of wood's most important physical properties, indicates the amount of actual wood substance present in a unit volume of wood. The density of a dry wood substance is 1.5 g/cc. Wood density depends on the species and varies from 0.2 to 1.2 g/cc. For example, balsa has an exceedingly porous composition and is extremely lightweight. Therefore, it is used for insulation, live-saving equipment, floats, biocomposites, and many novelties (Szatkowski and Chłopek 2021). Density also influences the mechanical properties of wood. Wood is a mechanically strong material, but the direction in which it is loaded in relation to the grain direction affects its strength. Wood loaded in

tension parallel to the grain is relatively strong, approximately 135 MPa for beech and 104 MPa for pine. The tensile strength of wood along the grain is about 2.5 times the compressive strength of wood. The bending strength of wood is lower than its tensile strength but higher than compressive strength. The bending strength in the direction of the grain is directly proportional to the density of the wood and may reach for softwoods 50 MPa and for hardwoods 70 MPa (Kollmann and Côté 1984; Gustafsson 2010). Wood has the ability to resist scratching and wear, which is called hardness. It depends on the density, moisture content, and anatomical direction and can vary by up to 50% within the same species (Holmberg 2000). Hard species are challenging to work with but are desirable for flooring or furniture.

Another property of great importance is thermal conductivity, which is relatively low because of the porosity of the wood. Therefore wood is commonly used as a thermally insulating material. For typical softwood lumber, thermal conductivity is in the range of 0.10–0.14 W/mK, i.e., much lower than the conductivity of steel (45 W/mK), and depends on the density, water content, temperature, or content of extractives (Ross 2021). Further properties providing information regarding the molecular structure of wood, wood–water interactions, and industrial application are electrical and dielectric parameters (Pentoś et al. 2017). Oven-dry wood is electrically insulating. However, electric resistance decreases as the moisture content increases, from 25,000 MΩ for a completely dry state (0% humidity) to 0.5 MΩ for the fiber saturation point (about 30% humidity).

As mentioned above, most of the properties of wood are affected by its moisture content. Wood is hydrophilic by nature. Water as a liquid or as vapor from the surrounding environment can be absorbed by the wood, changing its dimensions and density. Moisture in wood can affect decay and insect resistance and influence mechanical, thermal, and acoustic properties. Thus, many challenges in using wood as an engineering material arise from changes in moisture content. Wood is also flammable. This feature is utilized when the wood is used as fuel or in recycling. However, it also limits its use in many fields, especially in building construction. When heated, the wood undergoes thermal degradation and combustion to produce gasses, vapors, tars, and chars (Lowden and Hull 2013). Finally, wood can be affected by many abiotic and biotic factors—UV light, fungi, and insects—which can significantly contribute to wood discoloration, fracturing, and, finally, degradation, thus lowering the utilization value of wood (Kirker and Winandy 2014).

Currently, wood is used not only as raw material but also in many engineered forms, such as wood-based boards (WBBs), wood–plastic composites (WPC), or chemically and physically modified wood products. The formation of wood-based materials/panels enables the improvement of mechanical properties, maximizes the utilization of wood wastes, and decreases the price of products. The largest wood elements—lumbers are glued to form, e.g., cross-laminated timber or glued laminated timber, to improve mechanical properties or decrease the flammability of wood products. Thin wood slices—veneers are used to produce plywood or laminated veneer lumber, which can be used as structural panels. Other wood composites use smaller wood elements that often constitute wood wastes (e.g., wood chips, fibers, strands, etc.). These are used to manufacture oriented strand boards,

particleboards, medium-density fiberboards, etc. The other components of WBB are adhesives of sufficient binding strength. Finally, there are also boards in which wood in the form of wood flour constitutes a filler in a plastic matrix. The latter composites also often use other natural materials such as bamboo or straws (Kollmann et al. 1975; Yaghoobi and Fereidoon 2019; Pizzi et al. 2020).

Wood may also be processed physically or chemically to obtain materials of specific properties and functionalities. An example is the densification of wood by hot-pressing, which is intended to enhance the mechanical properties of wood (Laine et al. 2016). Chemical modifications may lead to the liquefaction of wood aimed at obtaining various value-added products, including activated carbon fibers (Zhao et al. 2019), coatings (Hochmańska-Kaniewska et al. 2022), fuels (Bhatwadekar et al. 2022), adhesives, etc. (Janiszewska et al. 2016; Sandak et al. 2018; Fernandes et al. 2022). Further, the wood may be chemically processed to obtain bioderived raw materials such as nanocellulose (Hochmańska and Janiszewska 2019; Liu et al. 2021). New literature also shows many examples of the formation of flexible wood aerogels (sponges) made by removing lignin and hemicellulose (Fu et al. 2020; Kumar et al. 2021). The remaining cellulosic structure is highly porous and elastic and thus may be used as a natural, biodegradable elastic scaffold for devices, sensors, or as membranes. Finally, thermally treated wood can go through various combustion routes, producing various chars that change the surface properties of wood (Kymalainen et al. 2017; Zhang et al. 2020). The thermal modifications can lead to the development of new materials, including different forms of carbon micro- and nanoparticles (Ishimaru et al. 2001, 2007; Xue et al. 2017).

This kinship of wood and carbon nanomaterials is quite interesting as carbon nanoparticles, particularly graphene and carbon nanotubes, are unique structures which had a huge impact on the development of materials engineering in recent years. Graphene is a single layer of sp^2 hybridized carbon atoms, i.e., carbon atoms are arranged in a hexagonal lattice where each atom forms three sigma

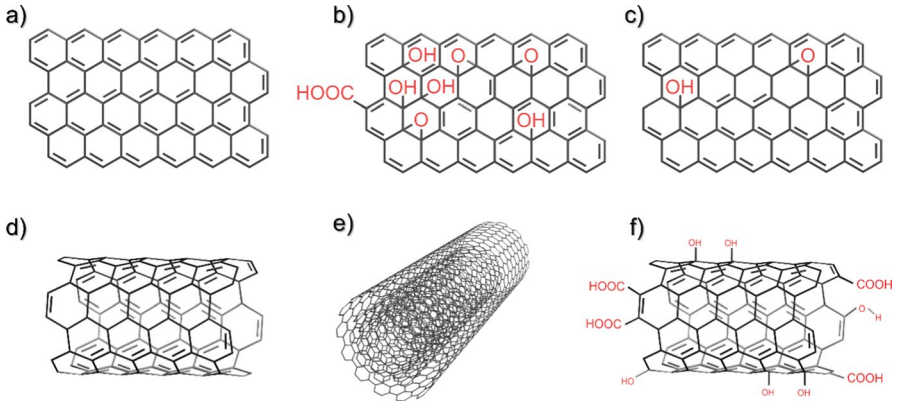

Fig. 1 Structure of **a** graphene, **b** graphene oxide, **c** reduced graphene oxide, **d** single-wall carbon nanotube, **e** multiwall carbon nanotube, **f** functionalized carbon nanotube. Reprinted from (Łukawski et al. 2022) under CC BY 4.0 license

bonds with its neighbors and has one pi orbital (Fig. 1a). This structure provides graphene with very high mechanical strength and stiffness and extremely high electrical and thermal conductivity (Allen et al. 2010; Novoselov et al. 2012). Additionally, graphene is very lightweight, hydrophobic, and chemically resistant. In practice, most types of graphene sold in the market have more than one layer and may have different diameters. Therefore, their properties may not reach those observed for single layers. Still, their performance is excellent for many applications. Up to this point, graphene was applied in electronics (e.g., nanocomponents, printed electronics), the energy sector (batteries, supercapacitors), as sensors, membranes, as well as fillers of many types of composites and coatings (Choi et al. 2010; Mohana et al. 2018).

Some graphene synthesis and post-treatment processes may result in the formation of graphene oxide—GO (Fig. 1b), a disordered graphene structure with epoxy bridges and hydroxyl and carboxyl functional groups (Dreyer et al. 2010). This structure is practically an electrical insulator and loses some mechanical properties. Still, it is also a hydrophilic structure that facilitates dispersion in water and uniform distribution in many polymeric matrices and coatings (Huang et al. 2012). The partial recovery of graphene properties is possible by reducing graphene oxide, which removes most functional groups and restores most sp^2-carbon–carbon bonds (Fig. 1c) (Pei and Cheng 2012). This form of graphene is treated as separate species from both graphene and GO and is referred to as reduced graphene oxide (rGO).

Carbon nanotubes (CNTs) are nanotubules with walls made of graphene. They may be synthesized as single-walled nanotubes (SWCNTs), i.e., with walls made of single-layer graphene (Fig. 1d) or multiwalled carbon nanotubes (MWCNTs) where several SWCNTs are encapsulated in each other (Fig. 1e) (Saito et al. 1998). Unlike graphene, nanotubes are 1D structures (they have nanosized diameters and most often nano- or micrometer lengths). Therefore, in composites, nanotubes form better percolation networks than graphene, but it is more difficult to obtain their high-loading fractions (Bauhofer and Kovacs 2009; Chen et al. 2020a). Their mechanical, electrical, and thermal properties along the length of CNTs are very similar to graphene (Brown et al. 2005; Koziol et al. 2007; Lekawa-Raus et al. 2017). They are also hydrophobic and chemically resistant (Lau et al. 2003; Janas et al. 2013; Saji 2021). Analogously to single and multilayered graphene, the properties of MWCNT may also be slightly poorer than the properties of SWCNTs. However, nanotubes, particularly MWCNTs, are at the moment much less expensive than graphene. Similarly to graphene and graphene oxide, better dispersion of CNTs in composites may be obtained using functionalized CNTs (Fig. 1f) (Tasis et al. 2006). Over the years, the research on CNTs focused on a wide range of applications in similar areas as in the case of graphene (Shoukat and Khan 2021).

Only recently, researchers have realized that graphene and carbon nanotubes could be successfully combined with wood and wood composites, not only improving the properties of the latter materials but also forming completely new structures and applications. A literature search performed by the authors shows that the number of scientific papers published per year increases sharply. Although it is still a very new area of research, it already covers many new ideas worth mentioning and analyzing.

This review aims to analyze the potential ways carbon nanomaterials (CNMs) may be combined with wood. It explores these two materials' interactions and analyzes the resultant materials' performance and their applications. The following review focuses on wood, processed wood forms such as wood sponges and biochars, and wood-based boards hybridized with CNMs. Due to the stronger similarity of WPC composites to polymer–CNM composites and the negligible interaction of wood and CNMs in WPCs, WPCs enriched with CNMs were described in a separate review (Łukawski et al. 2022).

Wood with graphene and carbon nanotubes

The number of publications concerning wood increased particularly sharply in recent years, showing that it has become a highly active area of research. It is also the most versatile area. Based on an in-depth analysis of the published papers, two major research directions may be distinguished. The first group of publications showed that CNMs might be effectively synthesized from wood and used either separately or in combination with wood substrates.

Next, studies used CNMs as functional coatings and impregnates of wood. These were used either to enhance/change the properties of wood or to produce novel applications and devices.

Synthesis of CNMs from wood

Wood is composed of carbon in 45–55% (Lamlom and Savidge 2003). The rest constitute oxygen (40–45%), hydrogen (4.5–6%), nitrogen (0.3–3.5%), and a trace amount of sulfur (Pettersen 1984; Dadile et al. 2020). All these elements are found in the feedstocks used to synthesize carbon nanomaterials. Depending on the synthesis process and targeted carbon nanomaterial, CNMs are synthesized from various carbon sources, including methane, acetylene, ethanol, natural graphite, etc. (Koziol et al. 2007; Sundaram et al. 2011; Lee et al. 2019; Bulyarskiy et al. 2020; Makgabutlane et al. 2021; Moosa and Abed 2021; Yu et al. 2021) These sources may thus contain not only pure carbon but also hydrogen, and oxygen atoms, which become by-products. Sulfur is also used in some synthesis processes to limit the growth of catalyst particles (Gspann et al. 2014; Yadava and Dasgupta 2020). Finally, nitrogen is most often introduced to synthesis processes to substitute carbon atoms in the carbon nanomaterial and form doped CNMs (Ewels and Glerup 2005; Boncel et al. 2014).

Thus, considering the composition of wood, it is a natural intuition to think of it as a natural substrate for the synthesis of CNMs. Indeed, many studies have found sp^2-bonded carbon structures in wood charcoal (Hata et al. 1998, 2000; Ishimaru et al. 2001, 2007). For example, the study of Murr et al. reported even finding carbon nanomaterials such as MWCNTs, fullerene-like structures, and graphite nanoplatelets in Texas piñon pine wood burnt in ambient conditions (Murr and Guerrero 2006). However, an interesting step further would be to work on the process

conditions to obtain targeted products of controlled parameters, e.g., only MWCNTs of specific lengths and the number of walls. In such a case, wood could become a highly promising natural, non-toxic, renewable substrate. Such research would become particularly interesting in the context of recycling wood waste.

Akhavan et al. (2014) demonstrated the synthesis of GO and rGO from wood waste. In this study black mulberry tree waste was tightly wrapped in aluminum foil and charred at ~ 400–500 °C for 5 days. The obtained material was ground by a mortar, again wrapped in aluminum foil and reheated at 450 °C for 24 h. Next the charcoal was graphitized by adding 1 g of charcoal and 0.5 g of $FeCl_3 \cdot 6H_2O$ to 100 mL of DI water. After pH adjustment by HCl, the suspension was stirred at 60 °C for 5 h, then left for 7 days at room temperature for gradual evaporation of water, and dried at 100 °C for 5 h. Next the material was ground again to obtain powder, used further to synthesize GO by modified Hummers' method. In this process 1 g of the powder was first suspended in 50 mL H_2SO_4 (80 °C, 24 h). Next, 1 g $NaNO_3$ was added to the suspension (ice bath, 1 h), followed by 6 g of $KMnO_4$ (4 h stirring in ice and at 35 °C for 1 h). Then the suspension was diluted by 100 mL DI water (< 60 °C) and, 6 mL of H_2O_2 (30%) diluted by 200 mL DI water. To remove residual acids and dissolved impurities, the suspension was centrifuged (8000 rpm, 30 min) and filtered through an anodic membrane filter was washed with DI water. This material was again dispersed in DI water and centrifuged (at 2000 rpm for 30 min and 8000 rpm for 60 min. Final GO suspension was achieved by ultrasonication of the above dispersion (40 kHz, 150 W, 30 min). To obtain rGO, the GO suspension was reduced by hydrazine. First, the pH of the GO suspension was adjusted to ~ 9 by diluted ammonia solution. Then, 35% hydrazine solution was added to the suspension and stirred at room temperature. Finally, the suspension was refluxed in an oil bath (90 °C, 3 h). This whole process was very complex but proved that CNMs may be synthesized from wood in a controlled way.

The next studies on CNM synthesis from wood were inspired by works on the formation of graphene from polymers via the use of lasers (example described by Huang et al. (2020a)). In this case, carbon rich polymers were treated with high-energy lasers which enabled the decomposition of polymer chains at the materials surface and the synthesis of a thin layer of graphene or graphene oxides depending on the synthesis conditions. Similarly, graphene was synthesized from wood.

Ye et al. (2017, 2018) proposed using an infrared CO_2 laser to produce porous hierarchical graphene. Woods used in this study included pine, oak, and birch. The samples were placed in a flow-through chamber and irradiated with a laser through the ZnSe window mounted on the top of the chamber. The synthesis was performed using a 10.6 mm CO_2 pulsed laser (75 W). It has been found that graphene, in the case of CO_2 laser, may be produced only in the reduced atmosphere; therefore, the synthesis was carried out under Ar and H_2 flow. The presence of oxygen caused ablation of the wood surface, decomposition of lignocellulose, and no graphitization. The experiment in which the laser power was tuned from 10 to 90% of laser power has shown that graphene structures start to form above 50% of laser power. Below 50%, only amorphous carbon is formed. The carbon layers were thin; at 70% power, the thickness amounted to 800 mm. The lowest sheet resistance amounted to 10 Ω/sq. The study also showed that high lignin content in wood facilitates the

formation of high-quality graphene. The authors also demonstrated some applications. The examples included a supercapacitor formed by the deposition of polyaniline onto the laser-induced graphene layer. The supercapacitor was characterized by a high areal-specific capacitance of ≈780 and ≈320 mF/cm^2 at current densities of 1 and 10 mA/cm^2. Other applications were water-splitting nanodevices formed by the deposition of either NiFe or CoP on the top of a laser-induced graphene layer. Both structures were able to catalyze the hydrogen evolution reaction and oxygen evolution reaction and work with high reaction rates at low overpotentials.

Trusovas et al. (2019) showed that graphene might also be produced on wood using solid-state near-infrared nano- and picosecond lasers. In this study, pine wood samples were placed in a nitrogen-filled chamber. The surface of the wood was irradiated through a sapphire window using a nano (10 ns) or picosecond (10 ps) laser beam of 1064 nm wave with a repetition rate of 100 kHz. The diameter of the focused beam amounted to 15 µm. The scanning speed was varied from 5 to 100 mm/s, and the mean laser power from 0.3 to 1.5 W. It has been demonstrated that the graphene film quality strongly depends on the laser irradiation dose. Therefore, neither too low nor too high doses were not beneficial for the graphitization process. The optimum dose for a nanosecond laser amounted to 662 J/cm^2. Sheet resistance for this dose reached the lowest value of 35 Ω per square. The dose for the picosecond laser, which produced minimum sheet resistance, was lower. However, in this case, a minimum sheet resistance reached 179 Ω/sq, which the authors attributed to the higher defectiveness of the graphene layer due to the higher temperature induced by picosecond lasers at the same fluence. Here, the minimum sheet resistance was higher than the one obtained by Ye et al. (2017, 2018) using a CO_2 laser. However, it is worth remembering that solid-state lasers are also characterized by lower power consumption, higher energy conversion efficiency, and better pattern formation precision due to shorter operational wavelength.

A significantly improved method of laser-induced graphene (LIG) synthesis was proposed by Le et al. (2019). Wood was converted to graphene in ambient air using a femtosecond UV laser (Fig. 2). The substrates used in the study included softwoods (pine), hardwoods (rosewood, bamboo, Narra padauk, basswood), and engineered woods (pressed wood, plywood). It has been found that short femtosecond pulses of high repetition rate (over 10 kHz) and high photon energy are able to cause carbonization and then graphitization even in the presence of oxygen. In such conditions, heat is not spread into surroundings but is localized in a targeted area, causing little ablation and efficient photoconversion. However, a decrease in the repetition rate below 10 kHz causes excessive heating and ablation observed before by Ye et al. (2017). The sheet resistance of the LIG layer was found to be dependent on both power and writing speed. Low writing speed (below 5 mm/s) at any power was found to cause high heat accumulation and high sheet resistance. An increase in the writing speed caused a decrease in the depth of conversion and first a reduction in sheet resistance and then its re-growth. The lowest sheet resistance was found to be 10 Ω per square, the same as Ye et al. (2017). The power of 0.8 W provided the lowest sheet resistance for the largest operational window for writing speeds. Although the highest power is necessary to obtain the best electrical parameters, approximately 10 times less energy is required to transform wood to LIG than a CO_2

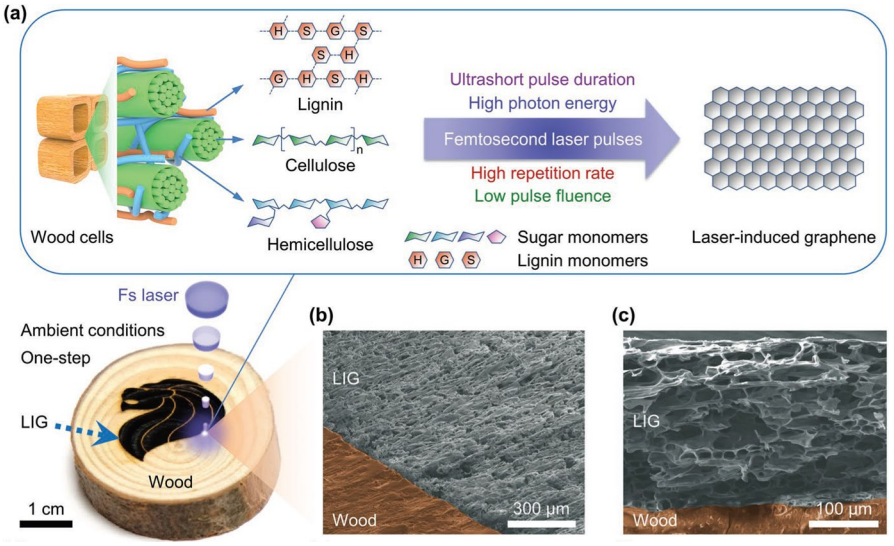

Fig. 2 **a** Process of formation of laser-induced graphene (LIG) from wood. **b** and **c** scanning electron microscope images of LIG on wood. Reproduced with permission (Le et al. 2019). Copyright 2019, John Wiley & Sons, Inc.

laser (Ye et al. 2017) (0.8 W vs. at least 6.3 W). The process is effective independent of the type of wood, indicating that all wood components (cellulose, hemicellulose, and lignin) are photoconverted to LIG just as efficiently. The method was applied to fabricate a printed-electronic circuit composed of interconnects, a resistor on wood, and a pseudocapacitor. The capacitor electrodes were manufactured by soaking wood in a $KMnO_4$ solution, drying them in air, and irradiating the samples with UV FS laser beam. The resulting MnO_2/LIG electrodes were sandwiched with Na_2SO_4 electrolyte and a tissue paper separator. The obtained capacitor showed an areal capacitance of 53.6 mF/cm^2 at 1 mA/cm^2.

Kim et al. (2021) used the femtosecond laser-induced graphene patterns to manufacture flexible thermistors (Fig. 3). To fabricate the thermistors Narra Padauk wood block was irradiated with a Yb-doped fiber femtosecond laser of 346 nm wavelength. Patterning resolution amounted to 40 mm. Once a graphene pattern

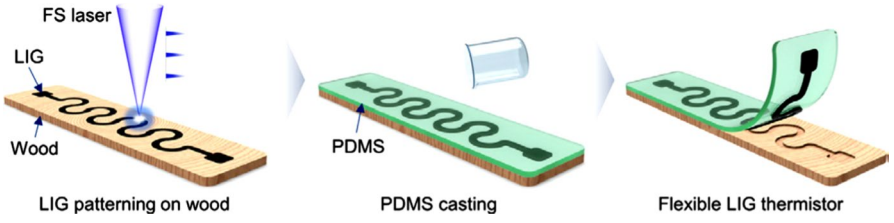

Fig. 3 Formation of flexible thermistor from lased-induced graphene. Image modified from Kim et al. (2021) with permission: copyright 2021, Elsevier

was scribed on wood, the overall wood surface was coated with a thin elastic film of PDMS of approx.0.5 mm. PDMS was prepared as a mixture of base and curing agent—weight ratio of 3:1. Upon curing at increased temperature, the graphene pattern was attached to PDMS. After solidification, PDMS with a graphene pattern was detached from the wood. The pattern resistance increased from an initial 0.5–29.5 kW after curing and detachment from wood, which was sufficient for the chosen application despite the increase. The proposed thermistor was found to have a positive temperature coefficient with a high sensitivity and temperature coefficient of resistance of 5.73% 1/°C. The fabricated thermistors were demonstrated to work well as temperature sensors on vacuum pumps, glass cups, and a human hand.

Fabrication of LIG electronic components and circuits by the above-presented pulsed laboratory lasers would be a very slow and expensive process. This is due to the cost of the equipment as well as the raster scanning mode of operation of these lasers. To tackle these issues Ishii et al. (2022) proposed manufacturing carbon electronic circuits on wood using a constant wave laser cutting machine. Laser cutting machines are low-cost laser equipment that operates in vector scanning mode. Depending on the power, beam focus and speed of operation it can be used for cutting or engraving various materials. The side product of the wood-cutting and engraving process is the formation of carbonaceous materials. The authors chose an engraving mode by setting power at 30–50% and high speeds of 381–457 mm/s. It was observed that to produce a sufficient amount of conductive carbon and obtain uniform coverage of the larger areas the laser had to be run 8–15 times over each region and the sample was set at 5–6 mm away from the laser focus. The lowest sheet resistance value obtained in this work amounted to 30 Ω/sq (uncoated wood) which is three times higher than in previous studies (Ye et al. 2017; Le et al. 2019). The authors did not present any analysis of the obtained carbon so it is possible that the carbon formed is a strongly oxidized graphene or carbon black. The reason for higher resistance may also be the non-uniformity of the pathways. It has been shown that in the case of some woods the paths were not conductive due to the formation of separated carbon islands. Based on this observation it has been concluded that the method works best for moderate hardness woods—lauan and Japanese cypress, but it is not suitable for hardwoods: beech, oak, walnut, and soft wood—cedar. It is also important to mention that every type of substrate requires some adjustment of the laser treatment parameters to obtain optimum results.

The synthesis of carbon nanomaterials from wood is a highly interesting topic. Although the cost and output of laser techniques are currently debatable in the context of large-scale applications, such studies open up a new area of research, which may, in future, develop into many more synthesis techniques.

Coating and impregnation of wood with CNMs

The authors of this review proposed a very simple method of combining wood samples with CNMs (Łukawski et al. 2018). Industrial grade MWCNT or graphene were suspended in dichloromethane and then deposited on wood by either dip coating or drop casting. High vapor pressure organic solvent quickly evaporated, leaving a

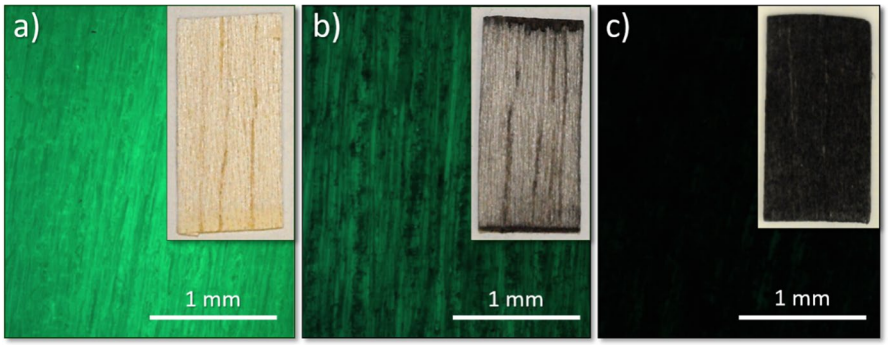

Fig. 4 Photographs of wood samples with the corresponding images from a fluorescence microscope (pure wood shows a fluorescence that is extinguished by the presence of CNTs on the surface) for **a** pure balsa, **b** balsa coated with CNTs once, and **c** 3 times. The CNTs were deposited via drop casting of 0.1% CNT suspension. Reproduced with permission from (Lekawa-Raus 2021)

visible thin layer of CNTs/graphene on the surface of wood samples (Fig. 4a, b). The low content of nanotubes (17 mg/l) and graphene (33–500 mg/l) used ensured homogeneous dispersion and uniform coating. However, several deposition repetitions were necessary to obtain full coverage (Fig. 4c). Similar coatings were prepared using water as a solvent. Water would be much easier to introduce into production lines in the wood industry. Due to the hydrophobicity of CNTs and graphene, in the case of water, it was necessary to use a small amount (0.3 wt.%) of surfactant—sodium dodecylbenzene sulfonate (SDBS), which was removed later by washing.

The most important result of this research was an observation that both CNTs and graphene show a firm adhesion to wood. They can be deposited in pure form, and there is no need to use any additional binders. The CNMs cannot be effectively removed by sandpaper treatment, and adhesion is independent of the type of wood (tests were performed on woods of differing porosity, cellulose, and lignin contents: balsa, birch, oak, poplar, pine, and beech woods). This phenomenon may be explained mainly by the significant cellulose content in all types of wood. Cellulose has been shown to have strong adhesion to CNMs (Shishehbor 2020; La Notte et al. 2018). The microporous structure of wood also facilitates the deposition and mechanical entrapment of nanostructures.

Additional observations from these studies show that such methods of CNMs deposition also cause infiltration of dispersion into the pores of wood and deposition of CNMs inside wood samples. However, the effect is visible only up to the depth of several hundreds of micrometers. The application of vacuum in our studies did not cause much deeper impregnation. Analysis of literature presented by other authors shows a very similar image. Even in a vacuum, bulk samples get only partly impregnated, and true impregnation is currently shown only for thin samples (up to several millimeters) (Goodman et al. 2018; Kim et al. 2019; Song et al. 2020; Wu et al. 2021). Song et al. who tested hydrothermally treated wood samples suggested that impregnation depth may be related to the surface state (hydrophilicity)

of tested samples (Song et al. 2020). It may be suspected that the impregnation will also be related to the dimensions of CNMs, their functionalization, or the impregnation method. This area needs some further studies.

Nevertheless, coating and impregnation studies already show interesting effects originating from a combination of wood and CNMs.

Superhydrophobic and hydrophilic coatings

The studies on wood coating showed that naturally hydrophilic wood coated with CNMs using drop casting and dip coating methods might gain highly hydrophobic or even superhydrophobic properties (Table 1) (Łukawski et al. 2018). Balsa wood samples coated with only 0.05 g/m^2 of MWCNTs or 0.25 g/m^2 of graphene showed a contact angle of nearly 150° over 140° and 130° for MWCNTs and graphene, respectively. Comparative tests performed using carbon black showed significantly lower contact angles. Although some variation of contact angles was observed for other than balsa types of wood, in all the cases, significantly increased contact angles were observed. All wood surfaces became highly hydrophobic when CNT or graphene coatings were applied. The hydrophobicity of the wood surface did not exclude the adhesion of water droplets to the surface, suggesting a "rose petal" type of hydrophobic behavior. Nevertheless, water absorption tests performed on wood fibers and particles coated with graphene showed a decrease in their water absorption by 98% and 87%, respectively.

It is well known in the literature that carbon nanomaterials can also form hydrophilic surfaces enabling the manufacture of many interesting applications (Saji 2021). Such coatings were formed on the wood surface using oxidized graphene (Huang et al. 2020a) and surfactants-enriched CNT suspensions (Łukawski et al. 2019a). Their applications are described in Sects. "Photothermal conversion efficiency and filtering capability - nanodevices" and "Electrical and thermal conductivity and electronic applications", respectively.

UV resistance

The study of Wan et al. (2015) (Table 1) showed that CNM coatings might significantly improve the UV resistance of wood. First, small poplar wood samples (20 mm × 20 mm × 10 mm) were pretreated by ultrasonication in the deionized water bath and drying in a vacuum. Next, the samples were immersed in an aqueous dispersion of GO and subjected to hydrothermal reaction in an autoclave, then rinsed and dried in a vacuum again. The spectrometry tests showed that after 600-h-long weathering tests consisting of exposure to fluorescent UV radiation, water spray treatment, and condensation process, the coated samples showed much less surface color and surface chemical composition changes than the original wood samples. The study also showed better thermal stability of the coated samples measured by TGA.

Table 1 Methods of combining CNMs with wood, studied properties and potential applications

	Composition	Deposition	Properties	Potential applications	References
1	A) graphene or CNTs B) SDS/CNT or SDS/graphene	A) Drop casting B) Dip coating followed by SDS rinsing	Hydrophobic/superhydrophobic properties	Water-repellant wood-based materials	Łukawski et al. (2018)
2	GO	Dip coating	UV resistance	Aging resistant wood	Wan et al. (2015)
3	MWCNTs, GNPs and lignin	Vacuum-assisted dip coating	Decreased flammability	Fire-resistant wood	Song et al. (2020)
4	Water-based acrylic-latex paint with graphene and Ni-based nanocrystals	Brush coating	Decreased flammability	Fire-resistant wood	Esmailpour et al. (2020)
6	Thermoset polymer with CNTs, and nanoclay	Vacuum-assisted dip coating	Improved mechanical strength	Enhanced wooden constructions	Hazarika and Maji (2014)
7	Waterborne PU with graphene	Spray coating	Improved mechanical strength	Enhanced wooden constructions	Xu et al. (2022)
8	A) SDBS/CNTs B) PMMA/CNTs C) CNTs	A) Spray coating B) Screen printing C) Spray coating	Implemented electrical conductivity	Heaters, sensors, antistatic surfaces, wood electronics	Łukawski et al. (2019a)
9	SDBS/ MWCNTs	Dip coating	Implemented electrical conductivity	Evaporation of organic solvents in wood	Kim et al. (2023)
10	SDBS/MWCNTs	Dip coating	Anisotropic electrical conductivity	Heaters, wood electronics	Kim et al. (2019)
11	GO	Vacuum-assisted dip coating followed by GO reduction	Anisotropic electrical conductivity	Heaters, wood electronics	Wang et al. (2021a)
12	Ferric chloride/GO	Fe^{3+} ions infiltration followed by vacuum-assisted dip coating in GO and GO reduction	Implemented electrical conductivity	Au catalyst in the electrochemical reduction of CO_2	He et al. (2023)
13	PVA with iron nanoparticles encapsulated in multilayered graphene	Vacuum-assisted dip coating	Increased thermal conductivity	Wood veneer for floor heating	Wu et al. (2021)
14	GO	Drop casting	Increased water evaporation rate	Water desalination by solar steam generation	Liu et al. (2017)

Table 1 (continued)

	Composition	Deposition	Properties	Potential applications	References
15	RGO/Fe/Ni (single layer)	Drop casting	Increased water evaporation rate and heavy metal-sorption	Water desalination by solar steam generation, heavy metal removal	Mehrkhah et al. (2021a)
16	RGO/Fe/Ni (double layer)	Drop casting	Increased water evaporation rate and heavy metal-sorption	Water desalination by solar steam generation, heavy metal removal	Mehrkhah et al. (2021b)
17	GNP/alkali lignin	Drop casting	Improved dyes absorption from water	Water purification	Goodman et al. (2018)

Thermal stability and flammability

Better thermal stability, as well as a decrease in the flammability of CNM-coated wood, was also observed by Song et al. (2020) (Table 1). The test specimens of western hemlock lumber (35 mm thick) were immersed in a dispersion of MWCNTs, GNPs, and lignin (ratio of MWCNTs to GNPs 2:1 and CNM-to-lignin ratio 1:2 by mass) and vacuum treated. Although the authors referred to this process as impregnation, further microscopy studies showed that CNMs entered the pores only up to several hundred micrometers. TGA tests showed that the presence of CNM/lignin coatings on wood surfaces decreased the temperature of the decomposition onset but simultaneously limited the amount of volatile gasses released and led to an increase in the amount of char residues. The samples exposed to open propane flame showed that the coating sped up the ignition but also delayed flame spread and improved the self-extinguishing properties of the samples. Cone calorimetry tests showed a decrease in time to ignition but also a reduction in the total heat release by 32%, CO_2 yield by 12%, and mass loss by 10% upon coating the samples. Unfortunately, the authors did not study the effect of lignin only, which is well known to possess fire retardant properties (Song et al. 2011; Vanska et al. 2016; Łukawski et al. 2020). Therefore, it is difficult to estimate how much of the effect is related purely to CNMs.

Esmailpour et al. (2020) tested the fire retardancy of wood coated with CNM-based materials (Table 1). In this work, beech wood specimens (5 mm thick) were coated with graphene composited with Ni-based nanocrystals (Ni, $Ni(OH)_2$, Ni-oxides). The coatings (190–200 mm thick) were performed with water-based acrylic-latex paint. Nanoparticles constituted 15 wt.% of the wet paint. Samples coated with Ni-graphene-enriched paint showed a 184% and 162% increase in time to ignition and glowing (the time after which the sample will show a flame or glowing that will last for at least a second), respectively, with regard to uncoated wood sample. Only paint-coated samples showed a slight decrease in both times. These results obtained for Ni-graphene-coated samples oppose those obtained by Song et al. (2020), which is probably related to the presence of Ni-based nanocrystals on the surface of graphene nanoplatelets. Ni-graphene-enriched coatings ensured a significant increase in back darkening time and back holing time decrease in burnt area and weight loss.

Improvement of mechanical properties

Two studies focused on the mechanical performance of wood and showed that CNMs might improve the mechanical properties of wood materials.

Lisyatnikov et al. (2020) proposed a method of strengthening wooden beams by reinforcement of their support areas with fiberglass and carbon nanotube–epoxy composites. Rectangular pine wood samples of 20 mm × 20 mm × 30 mm (along the fibers) were composited on two sides with face sheets made of epoxy resin reinforced with fiberglass (ED-20) and carbon nanotubes. The experimental variables included curing temperature (20, 40, and 60 °C), carbon nanotubes concentration (0.1, 0.3, and 0.5%), and several facesheet layers (1,3, and 5). The compression tests (across the fibers) showed that all facesheets improved the mechanical performance

of the samples. The highest increase in strength of 39% was obtained for samples with five layers of the composite cured at 60 °C and comprising 0.3% of CNTs.

Hazarika and Maji (2014) improved the mechanical properties of fig tree wood samples by their impregnation with thermoset polymer, CNTs, and nanoclay (Table 1). Before impregnation, wood samples were pretreated in a vacuum to remove air from the pores. Next, they were immersed in a prepolymeric mixture of a copolymer of melamine formaldehyde and furfuryl alcohol (MFFA), furfuryl alcohol–water (FA-water), maleic anhydride, and 1,3-dimethylol 4,5-dihydroxy ethylene urea (DMDHEU) crosslinking agent. Some mixtures were enriched with 3 phr nanoclay and 0.5–1.5 phr MWCNTs functionalized with OH groups. The samples were kept in a vacuum for 6 h, then cured at 90 °C and cleaned from any remaining homopolymers. It has been found that impregnation with raw polymers significantly increased the weight and volume of the samples. The addition of nanoclay increased these parameters slightly more, while MWCNTs-OH had little effect on weight and volume. However, the presence of MWCNTs-OH caused the most significant increase in the hardness of the samples. XRD analysis of raw and composite samples showed a decrease in the crystallinity of cellulose chains upon impregnation. DMA tests indicated that the addition of nanoclay and MWCNTs-OH significantly increased dynamic modulus, which was attributed to decreased mobility of polymer chains. Simultaneously, their presence increased loss modulus related to impeded relaxation processes. However, in total, the damping parameter decreased in the presence of nanoclay and MWCNTs. Flexural and tensile tests showed that all additives improved mechanical performance. However, the most pronounced increase in flexural and tensile strength and stiffness was observed for CNTs, especially 1.5% MWCNTs. Finally, both nanoclay and MWCNTs significantly decreased the water uptake of the samples.

A recent study by Xu et al. (2022) showed that CNMs may also improve the mechanical properties of wood coatings (Table 1). The authors focused on waterborne polyurethane paints used often in furniture applications. Various contents of graphene oxide (0, 0.05, 0.1, 0.4, 0.7 and 1 wt% based on the solid content of PU) were mixed with aqueous PU prepolymer. The paints were tested in the form of self-standing films and after coating on maple veneer. The veneer was first coated with sealer primer and primer twice, cleaned with sandpaper, and spray coated with GO-polyurethane paint. It has been shown that the optimum content of GO amounts to 0.1 wt.%. For this content tensile strength, abrasion resistance, and pendulum hardness increased by 62.23%, 14.76%, and 12.7%, while slightly improving other properties such as solvent, water or alcohol resistance.

Electrical and thermal conductivity and electronic applications

The superhydrophobic CNM coatings presented by Łukawski et al. (2018, 2019a) (Fig. 4) were observed to render the wood surface electroconductive (Table 1). Even single, partly transparent coatings exceeded the percolation threshold and thus could be applied as antistatic coatings. Multilayered coatings reached conductivities that could well be used in electronic applications. Pure nanocarbons on wood substrates are perfect candidates for producing microscale green electronics components (Zhu

et al. 2016; Le et al. 2019). However, this combination of materials may also create many large-scale electronic applications such as large-area floor heaters, indoor flood sensors, indoor motion sensors, drying systems for wooden houses foundations, control systems for cracks in roof trusses, etc. The latter area was investigated in Łukawski et al. (2019a). The work focused on measurements of the electrical conductivity of CNM coatings performed using printed electronics techniques and the construction and testing of sensors and heaters, which could be used in wood construction and interior furnishings. Printed electronics techniques enable the mass production of inexpensive micro and macroscale electronic components. Printing is a fast process that does not require highly controlled ambient conditions. The components may be formed on almost any substrate, including flexible foils, textiles, or paper. Unlike the dip coating and drop casting techniques, the printed electronics methods allow for easy coating of selected surfaces and formation of patterns with the aid of stencils while simultaneously providing better control of the amount of applied material.

The tests on antistatic coatings prepared via spray coating of aqueous dispersions of MWCNTs (with SDBS) showed that the percolation threshold for MWCNT coatings on wood is achieved for a minimum of 7.8 ± 0.9 μg/cm^2 of CNTs. Further increase in the amount of material by application of subsequent layers reduces the resistance along with the number of layers. This is consistent with the reduction in resistance with parallel connection of resistors with the same resistance value. Similar conclusions were valid for coatings made with organic solvents-based inks (spray coating technique) and for coatings applied by screen printing through the stencil (paste formulation—MWCNTs dispersed in an 8% solution of polymethyl methacrylate in diethylene glycol butyl ether acetate; Janczak et al. 2014; Lepak et al. 2018)).

These base results enabled the design and construction of wood electronic components, which included water and organic solvent sensors, pressure sensors, temperature sensors, heaters, and dryers (Fig. 5) (Łukawski et al. 2019a).

The most effective liquid sensors were obtained via coating wood with MWCNTs using the spray coating technique and aqueous dispersions of MWCNTs with SDBS. The addition of SDBS rendered the coatings hydrophilic, which facilitated the influx of water into the MWCNT network, and it was possible to measure a change in the resistance of the coating. Such structures may be used as flood sensors. Raw MWCNT coatings applied by spray coating technique were found to change resistance linearly with applied temperature, indicating that such coatings could be used as temperature sensors to control ambient conditions or fire protection systems. The pressure sensor was constructed from two pine boards. The smooth surface of the CNT/PMMA-coated board faced with the rough surface of the CNT/SDBS-coated board enabled a formation of a stress sensor which changed resistance linearly with applied pressure. Such sensors applied under decorative flooring layers could be a base for indoor motion detection systems. Finally, it was demonstrated that screen-printed thick films of CNT/PMMA were the most uniform in terms of electrical conductivity and thus enabled the formation of reliable heaters. Such heaters could heat indoor spaces or dry up wooden constructions. Simultaneously, the study showed

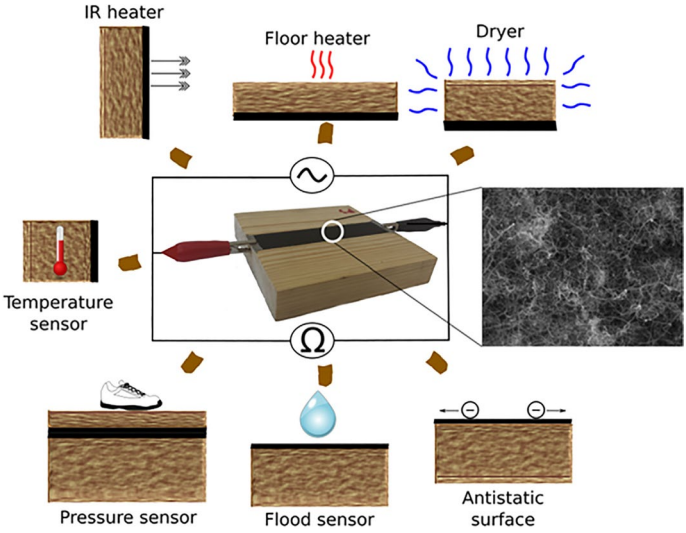

Fig. 5 CNM electronic components integrated with wood. Reproduced with permission (Łukawski et al. 2019a). Copyright 2020, Elsevier

that the cost of such integrated electronic components is very low, and the coatings could be produced using graphene instead of CNTs.

The versatility of uses of CNM wood coatings was additionally confirmed by Kim et al. (2023), who adopted the methodology of liquid sensors formation presented by Łukawski et al. (2019a) to study the absorption and evaporation of organic solvents in wood (Table 1). Kim et al. coated walnut wood samples (0.1 cm × 6 cm × 6 cm) with MWCNTs by dipping them for 10 s in the aqueous dispersion of MWCNTs (0.05 wt.%) and SDBS (0.5 wt.%). The samples showed an average resistance of 4676 Ω in an axial direction and 166,440 Ω in a tangential direction. Next, a DC voltage of 5 V was applied to the samples in the axial direction. The current was measured (along the sample) upon deposition, absorption and evaporation of 100 µl large droplet of every tested solvent. Altogether four polar solvents (water, acetone, ethanol, and isopropanol) and three non-polar solvents (n-hexane, benzene, and toluene) were studied. In all the cases a clear exponential decrease of current was observed upon absorption of the solvents and exponential increase upon evaporation. The correlation between polarity and the absorption and recovery times is not clear, however, some very interesting observations can be listed. For example, the time of absorption (i.e., for the current to reach minimum) was the shortest for acetone (20 s) and n-hexane (16 s) and the longest for water (401 s).

The same authors also studied wood impregnation (Table 1) (Kim et al. 2019). The authors used similar walnut wood samples (0.1 cm thick) and aqueous MWCNT/SDBS dispersion, but repeated the dipping procedure 7 times. It has been shown that repeatedly dipped samples show much lower resistances but still a clear difference in conductivity between axial and tangential directions. The resistance in the axial direction amounted to 45 Ω, and for the tangential direction, 748 Ω. A clear

difference was also observed when the same voltage was applied in both directions, and equipotential lines were determined.

Further studies also showed that thin wood samples might be impregnated with CNMs and become conductive electrically and thermally, which may also be interesting for many electronic applications.

A study by Wang et al. (2021a) reported on preparing conductive wood structures by impregnating wood with rGO (Table 1). First, poplar wood samples were dehydrated and mixed with GO. Next, the mixture of wood and GO was subjected to a pulsed vacuum and dried. Finally, ascorbic acid was applied to reduce GO, and the sample was dried again. The authors observed a decrease in the pore size of the impregnated wood and better thermal stability measured by TGA. The conductivity of samples was also anisotropic, with the lower resistivity measured in the cross section of the wood sample (resistivity in cross section—36.7 Ω cm, in radial direction—591.4 Ω cm, and 3231.3 Ω cm in tangential direction). The cross section was also found to have the highest carrier concentration out of all three directions.

He et al. (2023) showed that rGO-impregnated wood may be used in practical applications (Table 1). In this study, Chinese fir wood was cut into circular pieces of 5 mm diameter and various thicknesses (40, 80, 100 and 200 µm). The samples were degreased by 24-h-long treatment in 3.75 mol/L NaOH solution and washed with DI water. Next, the samples were immersed in 2 mol/L ferric chloride solution for 24 h and then washed. In this way, wood was infiltrated with Fe^{3+} ions and thus positively charged. The positive charge was used to increase the deposition of GO within the structure thanks to the electrostatic interaction between Fe^{3+} ions and GO. The samples were impregnated with GO by immersion in 150 g/L GO solution, vacuum treatment, washing, and freeze-drying. The reduction of GO was performed by 6-h-long immersion in 2 mol/K potassium borohydride solution. Finally, the samples were freeze-dried again. The authors showed that 40 µm thick samples prepared by the above procedure showed the lowest resistance which amounted to 2.01kΩ. Any changes in the protocol such as the omission of the first freeze-drying process or lack of deposition of Fe^{3+} ions are detrimental to the electrical conductivity of the samples. In agreement with the results of previous studies (Kim et al. 2019; Wang et al. 2021a) the lowest resistance was observed along the direction of the pores and the highest at a 90° angle from the tangential direction. The resistance was also decreasing with decreasing thickness of the sample and number of impregnations (up to 3 rounds were tested). Finally, it has been shown that the obtained samples can be successfully used as a replacement of carbon paper substrate for Au catalyst in electrochemical reduction of CO_2. It has been shown that in the reaction, the CO selectivity was increased as compared to both Au and Au deposited on carbon paper. The total current density of the substrate was several times greater for both reference substrates. Simultaneously, the selectivity of hydrogen evolution reaction (HER) was inhibited.

Wu et al. (2021) focused on thermal properties and tested the possibility of improving the thermal conductivity of wood veneers by their impregnation with graphene-based material and polyvinyl alcohol (Table 1). Two-mm-thick fast-growing poplar veneer was impregnated with PVA solution in water with iron nanoparticles encapsulated in multilayered graphene (0, 1, 2, 3 wt.% of PVA solid content). In

total, 12 impregnating formulations were tested. The impregnation process was performed in a vacuum. It has been shown that some of the formulations can improve the samples' thermal conductivity. The most effective was 10 wt.% of PVA and 2 wt.% of multilayered graphene-encapsulated iron. This formulation gave thermal conductivity of 0.22 W/mK, which was 2.4 times more than for untreated veneer. TGA studies also showed slightly better thermal stability of PVA and PVA-Fe-graphene-treated samples.

Photothermal conversion efficiency and filtering capability—nanodevices

Coating wood with carbon nanomaterials also enabled the formation of nanodevices for solar steam generation and water purification. With the increasing problems of water scarcity, the design of water purification and desalination systems has become a very widely studied topic (Gehrke et al. 2015; Lin et al. 2019). A combination of natural wood and CNM coatings turns out to be highly effective in this respect. The natural capillaries of wood are designed by nature to transport water, while CNMs are very effective in the absorption of sunlight. When wood is placed on the water surface with capillaries perpendicular to the surface and coated on the top with CNMs, solar energy is very efficiently captured by the CNM layer. The CNMs layer generates heat leading to water evaporation at the water–air interface. The low thermal conductivity of wood does not allow heat dissipation increasing the efficiency of the process. Simultaneously, the negative pressure forced by the evaporating water induces capillary forces in the wood nanochannels, lifting further water for the process. Additionally, purpose-designed CNM coatings may form effective filters.

Huang et al. (2020a) prepared the device by coating the top and bottom part of the wood sample (balsa, pine) with thermoplastic polyimide, which was irradiated with a 10.6 μm CO_2 laser (Fig. 6). First, the top surface was irradiated in an oxygen-free nitrogen atmosphere turning PI into graphene. Next, the bottom polyimide-coated surface of the wood was irradiated in the air forming highly oxidized graphene structures with hydrophilic properties. The tests showed that such nanodevices could reach a solar energy conversion efficiency of 110%. The upper hydrophobic layer also is very efficient in desalinating the water vapors and stopping salt from deposition on the top of the device. At the same time, the bottom hydrophilic layer was antibacterial and very effective in the filtration of organic compounds. The authors also showed that the evaporation rate might be augmented by the increase in pore diameter in wood, while the length of pores (thickness of the wood sample) affects thermal management.

Liu et al. (2017) showed that the steam generation and desalination effects might be obtained using graphene oxide layers deposited by drop casting, a much simpler and less expensive deposition method (Table 1). In this study, aqueous GO dispersion (0.3 wt.%) was drop-cast on the top surface of radially cut basswood samples. It has been shown that the evaporation efficiency of the wood − GO amounted to 82.8% at a power density of 12 kW/m^2 compared to raw wood evaporation efficiency, which was approx. 59.5%. The calculated steady-state evaporation rate of

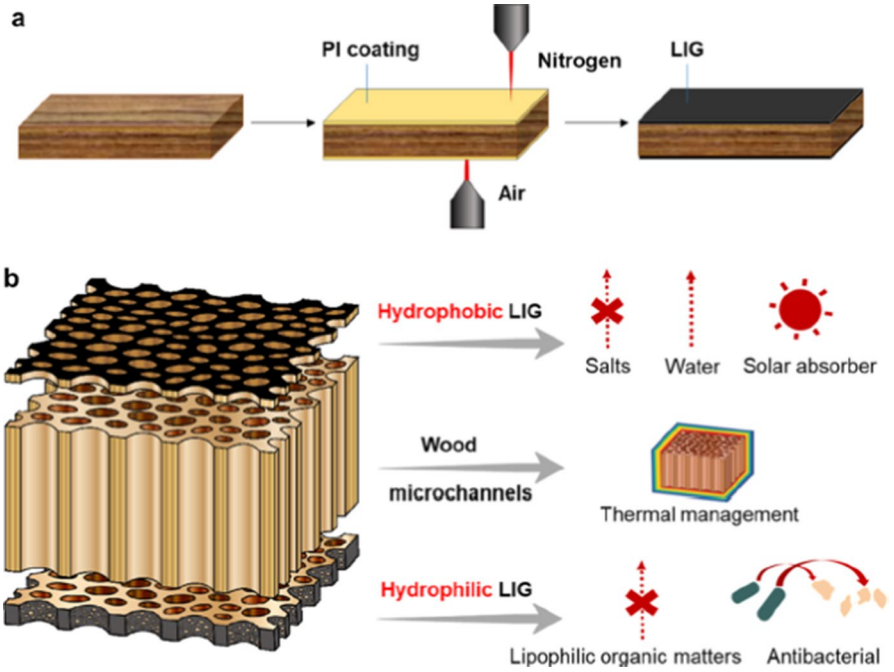

Fig. 6 **a** Formation of hydrophobic and hydrophilic lased-induced graphene (LIG) wood coatings by laser irradiation of thermoplastic polyimide (PI) coatings in nitrogen and air atmosphere, respectively. **b** Structure and operation of wood-LIG-based device for steam generation and water purification. Reprinted with permission from Huang et al. (2020a). Copyright 2020, American Chemical Society

the GO-coated samples over 200 s of irradiation (12 kW/m^2) amounted to 14.02 kg/m^{2}h, while for pristine wood 10.08 kg/m^{2}h.

Mehrkhah et al. (2021a) modified the steam generation system by coating the wood with iron/nickel-reduced graphene oxide nanocomposite, which, apart from steam generation and desalination, enabled heavy metals sorption (Table 1). In this work, nanocomposites of Fe/Ni bimetal and rGO with various starting concentrations of rGO (rGO prepared from either 100, 200, or 400 mg of graphite oxide in 400 mL of DI water) were deposited on poplar wood samples. The best performance was obtained for rGO200. This nanodevice reached evaporation fluxes of 1.43 and 4.19 kg/m^{2}h under 1 and 3 sun (1 sun = 1 kW/m^2) and decreased the salinity of water by four orders of magnitude. It also removed 100% of Pb (II) from 20 mg/L aqueous solutions within 40 min and 83.33% from 30 mg/L solutions. Further study by the same authors (Table 1) showed that separating Fe/Ni bimetal and rGO coatings provides better results (Mehrkhah et al. 2021b). Thanks to the deposition of Fe/Ni bimetal on the top of the device and rGO at the bottom, the evaporation rates increased to 1.5 and 4.77 kg/m^{2}h under 1 and 3 suns, respectively.

Ebrahimi et al. (2022) proposed coating of poplar wood samples with rGO and silver nanoparticles (Ag NP) (Table 1). The active layer was formed by drop casting of rGO dispersion in water with concentrations of 20, 40, 80, and 100 mg/mL and aqueous dispersions of Ag NP with concentrations of 20, 40, 60 and

80 mg/mL. The optimum sample, made with 80 mg/mL dispersion of rGO and 80 mg/mL of Ag NP, reached an evaporation rate of 5.99 kg/m^{2}h under 3 suns and 3.71 kg/m^{2}h under 1 sun. Thanks to the presence of Ag NPs, the devices also showed antibacterial properties.

Finally, Goodman et al. (2018) focused only on the filtering effect and showed that basswood cylinders coated with GNPs could filter water from dyes (Table 1). GNPs were dispersed in water with alkali lignin as a surfactant. The dispersion was then drop cast on basswood samples of 6 mm thickness and vacuum treated. Next, the samples were cut in half to obtain 3-mm-thick filters. The filtering tests performed using methylene blue showed that high uptake capacities characterize the filters up to 46 mg/g. Finally, the filters were tested for potential recovery. The best results were obtained for acetonitrile exchange which gave regeneration efficiency of over 80%.

Processed wood materials with carbon nanomaterials

Applications of carbon nanomaterials combined with processed wood materials are recently a flourishing topic. Most of the literature focuses on "wood sponges," prepared by delignification and partial or full removal of hemicellulose. Such wood is highly flexible while remaining natural, biodegradable, and, in many cases, highly porous. Up to now, "Wood sponges" enriched with CNMs have been mostly applied as green electronics components, flexible nanodevices for steam generation and filtration of seawater, and phase change materials. Other processed wood materials mentioned in the literature are biochars. The hybridization of CNMs with biochars was used to improve the adsorption properties of the latter ones and form electrodes for supercapacitors.

Wood sponges

The processes of manufacture of base wood sponges and flexible CNM–sponge composites were similar for most works (Guan et al. 2020; Cai et al. 2021; Huang et al. 2021; Sun et al. 2021; Wang et al. 2021b; Zhang et al. 2022). Thin balsa wood specimens (800 µm–10 mm thickness) of various sizes were usually soaked in sodium chlorite ($NaClO_2$) to remove lignin and then in a sodium hydroxide (NaOH) to extract hemicelluloses (Guan et al. 2020; Sun et al. 2021; Wang et al. 2021b). Sometimes, sodium chlorite was replaced by sodium sulfite (Na_2SO_3) (Cai et al. 2021; Zhang et al. 2022), and soaking in NaOH was replaced by boiling in H_2O_2 (Goodman et al. 2018). Some samples were vacuum-treated to improve the extraction process. Next, all samples were freeze-dried, which caused the formation of highly porous sponges. Afterward, the sponges were infiltrated with CNMs, usually soaking in the aqueous or organic solvent

solutions containing CNMs. When GO was used, it was hydrothermally reduced, using hydroiodic(Guan et al. 2020) or ascorbic acid (Huang et al. 2021).

Electronic applications

The research in the electronics area included studies on the formation and electrical performance of wood sponges hybridized with CNMs and the construction and testing of pressure and gas sensors.

Sun et al. (2021) proposed a method of manufacturing conductive wood sponge composites. The sponges were prepared by standard procedure ("Wood sponges") and infiltrated with MWCNTs functionalized with COOH groups. The sponges were hot-pressed to obtain MWCNT/cellulose hierarchical composites. The authors reported that the conductivity of the specimens increased with the concentration of MWCNTs and was anisotropic. The highest conductivity was measured for a 4 mg/mL concentration of MWCNTs and amounted to 132.42 S/m along the fiber direction and 43 S/m across the fiber direction. Tensile properties also increased with the addition of MWCNTs and were anisotropic. In all cases, the mechanical properties improved compared to pristine wood. However, they decreased with the content of MWCNTs, probably due to the agglomeration of CNTs. The tensile strength for the most conductive samples (4 mg/mL) amounted to 66.07 MPa in the fiber direction and approx. 7 MPa across the fiber direction. All samples were highly flexible. Potential applications of the proposed composites are listed in Table 2.

Wang et al. (2021b) used delignified wood filled with CNT and $Ti_3C_2T_x$ MXene to produce lightweight, elastic, conductive composites for wearable electronics applications (Table 2). Additionally to a standard procedure, the samples were vacuum impregnated with polydimethylsiloxane (PDMS) to improve their mechanical properties and protect them from harsh environments. After curing of PDMS, four types of samples were obtained differing with CNT/MXene weight ratios—0:1, 1:1, 2:1, 3:1. It has been shown that the addition of MWCNTs increased electrical conductivity of the samples with the highest value of 9.8 S/cm recorded for 2:1 CNT/MXene weight ratio. These samples also showed the best shielding performance of up to 29.3 dB. The samples were also hydrophobic, and their contact angle did not decrease after various treatments, such as abrasion tests or immersion in acid. Compressive stress and strain tests showed apparent differences in the performance along and across the fiber growth direction, indicating that any wearable electronic device should be designed to work across the direction of the fibers due to much larger strains measured. Independent of the direction, the composite's formation improved the cellulose scaffolds' compression performance, giving 1.53 MPa and 74.1% for perpendicular compressive stress and strain, respectively. The cyclic tests at a constant strain of 30% and 60% showed very good repeatability. Finally, a composite was successfully used as a pressure sensor to monitor human motions.

Zhang et al. (2022) produced elastic electronic components by combining flexible wood scaffold, MWCNTs, silver nanoparticles (Ag NPs), and poly(3,4-ethylenedioxythiophene)–poly(styrenesulfonate) (PEDOT:PSS). The flexible wood samples were infiltrated with MWCNTs pretreated with nitric acid and then freeze-dried. Next, the Ag NPs were deposited by infiltration of the FW/MWCNTs samples

Table 2 Potential applications of wood sponges and wood-derived biochars coated with CNMs

		CNM	A major influence of CNM addition	Potential applications	Publication
Wood-derived sponges	Electronic applications	MWCNTs	Improved electrical conductivity (from 10^{-7} to 10^{2} S m^{-1})	Conductive circuit (potentially sensors, electromagnetic interference shielding, and smart packaging material)	Sun et al. (2021)
		MWCNTs and MXene	Increased electrical conductivity shielding performance Hydrophobic	Pressure sensor to monitor human motions	Wang et al. (2021b)
		MWCNTs + Ag NP + PEDOT:PSS	Area capacitance 266.7 mF/cm2 at 20 mV/s 970 dB cm^2/g	Flexible supercapacitor electrode EMI shielding antibacterial properties	Zhang et al. (2022)
		rGO	A high sensitivity stability over 10 000 cycles, Fast response time (150 ms), Low detection limit (60 Pa)	Flexible pressure sensors	Guan et al. (2020)
		P-rGO	Water contact angle of 152° High sensitivity up to 4.93 kPa^{-1} in 0–5 kPa A fast response time of 160 ms	Piezoresistive pressure sensors for detecting human motions	Huang et al. (2021)
		SWCNT	Excellent stability under high humidity (75%) and low temperature (− 18 °C),	Self-powered triboelectric nanogenerator as Gas sensing system for food quality assessment	Cai et al.(2021)
	Nanodevices and phase change materials	F-rGO	Water contact angle of 145° Separation efficiency of 99%	Crude oil clean-up device	Huang et al. (2020b)
		CNTs	Thermal conductivity of 0.21 W/mK 0.950 kg/m^2h under 1 sun	Solar steam generation device	Chen et al (2017)
		rGO + polypyrrole	1.49 kg/m^2h under 1 sun	Solar steam generation device	Wong et al. (2023)
		rGO	2.26 kg/m^2h under 1 sun 22.6 mV and 144 μA at 36.2 °C	Solar steam generation electricity generation	Li et al. (2023)
		CNTs	Thermal conductivity 0.9832 W/(m·K) Latent heat 230.3 J/g at 119.7 °C	Phase change materials	Qin et al. (2021)
		rGO	Latent heat 218.5 J/g at 42 °C	Phase change materials	Huang et al. (2022)

Table 2 (continued)

	CNM	A major influence of CNM addition	Potential applications	Publication
Wood derived biochars	Graphene	20 times higher adsorption capacity than that of the unmodified cotton wood biochar (174 mg g − 1)	PAH adsorbant	Zhang et al. (2012)
	MnO_2/GQDs	Excellent cycling stability (95.3% retention after 2000 cycles)	Supercapacitors (energy storage devices)	Zhang et al. (2020)
	Graphene	Adsorption capacity**:** 18.4 mg/g	Cu^{2+} adsorbant	Samaraweera et al. (2021)
	CNTs	CNTs were grown on the charred wood by the CVD method The areal capacitance of 1940 mF/cm^2	Supercapacitor electrodes	He et al. (2022)
	CNTs	CNTs were grown by the CVD method during the charring of wood Specific capacitance of 6620.3 mF/cm^2, Gravimetric capacitance 118.5 F/g Volumetric capacitance 82.8 F/cm^3 at 2 mA/cm^2	Supercapacitor electrodes	Yan et al. (2023)

HI—hydroiodic acid, F-rGO—fluoroalkyl silane modified reduced graphene oxide, P-rGO—PDMS modified reduced graphene oxide, PAH—polycyclic aromatic hydrocarbons, MnO_2—manganese dioxide, GQDs—graphene quantum dots

with the solution of $AgNO_3$ in dimethyl sulfoxide and trisodium citrate dihydrate. The washed samples were next soaked in PEDOT:PSS solution and dried. The PEDOT:PSS samples showed the highest conductivity which amounted to 1.21 S/m and the good specific EMI shielding effectiveness of 970 dB cm^2/g. It has been shown that FW/MWCNT/Ag/PEDOT:PSS were characterized by very good flexibility. They also remained porous thus breathable and useful for supercapacitor applications. When used as supercapacitor electrodes they showed an area capacitance of 266.7 mF/cm^2 at 20 mV/s and long-term cycling stability of 84.3% capacitance retention after 5000 cycles at 5 mA/cm^2. Additionally, thanks to the presence of Ag NPs the samples were shown to be antibacterial.

Guan et al. (2020) and Huang et al. (2021) constructed flexible pressure sensors (Table 2). Guan et al. (2020) prepared ~800 µm-thick flexible wood (FW) samples coated in rGO. The FW/rGO was assembled on top of an interdigital electrode to obtain a flexible pressure sensor. Upon application of pressure, the contact resistance of the sensor decreases, as shown in Fig. 7. The sensors were produced as individual and array structures. The sensors were characterized by a fast response time of 150 ms, a low detection threshold of 60 Pa, high stability at cyclic loading and high sensitivity (1.85 1/kPa over linear range of 0–60 kPa). The sensors were demonstrated to successfully detect human motions.

Huang et al. (2021) manufactured pressure sensors from relatively large balsa wood samples (10 mm × 10 mm × 10 mm). After the standard delignification procedure, the samples were coated with GO, reduced, then immersed in 1.5 wt.% PDMS/hexane solution and cured. To obtain pressure sensors, the sponges were connected to 2 copper electrodes using silver paste (sensors were used as self-standing

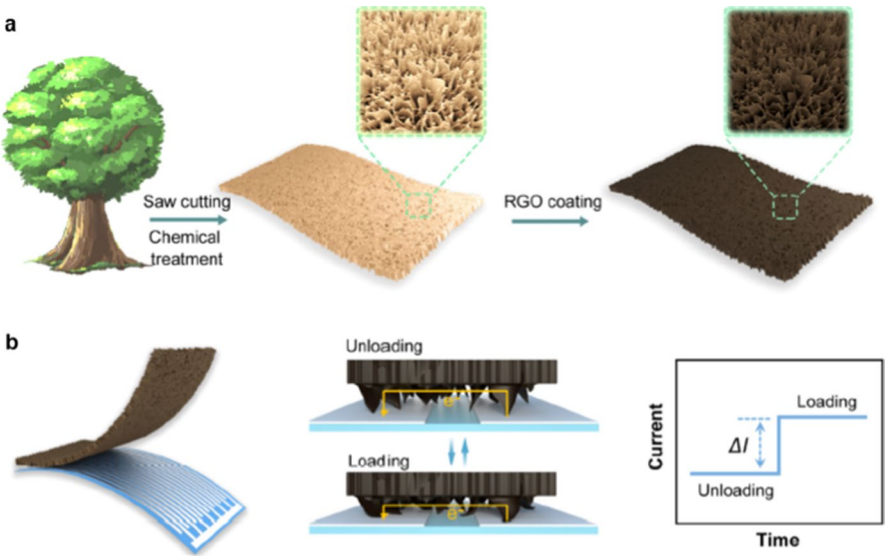

Fig. 7 **a** Formation of flexible wood (wood sponge) coated with rGO. **b** Construction and operation of a flexible pressure sensor. Reproduced with permission from Guan et al. (2020). Copyright 2020, American Chemical Society

structures). Upon compression, a decrease in resistance was recorded. The tests showed that the rGO-coated sponges were superhydrophobic and highly resistant to fatigue also in humid conditions. The sensors had a fast response time of 160 ms, similar to the one reported by Guan et al. (2020). The sensitivity of these sensors was higher than for the previous study (4.93 1/kPa compared to 1.85 1/kPa for Guan's et al. study); however, over a much shorter range of 0–5 kPa, in the further range of 5–50 kPa, the sensitivity dropped to 0.75 1/kPa. Nevertheless, they were shown to detect human motions successfully.

Cai et al. (2021) used CNT-enriched conductive flexible wood to produce a gas sensing system for food quality assessment (Table 2). The system used gas sensing properties of CNT which change conductivity upon exposure to many gasses, including ammonia, the primary marker of food spoilage as well as a triboelectric effect (Panes-Ruiz et al. 2018; Han et al. 2019; Norizana et al. 2020). Conductive FWs were combined with a film of fluorinated ethylene propylene (FEP) to produce a nanogenerator. Both films were sandwiched between copper sheet electrodes connected to external circuitry measuring the output signals. The system was also equipped with a wireless module to transmit data to the user. The operation of the nanogenerator was based on the triboelectric effect. Upon compression of the nanogenerator and contact of FEP and wood, FEP gains a negative charge while wood becomes positively charged. When the layers separate potential difference arises in the generator causing electric current to flow until the full separation of layers is obtained. Upon recurring compression, current flows in the opposite direction until full contact of layers is obtained. When CNT-enriched wood came into contact with ammonia, its conductivity increased, changing the amplitude of the voltage and current of the triboelectric nanogenerator. It has been shown that the system could measure ammonia concentrations from 50 to 500 ppm and work at low temperatures of − 18 °C and in high humidity of 75%.

Nanodevices and phase change materials

As mentioned above, wood aerogels have also been the basis for constructing nanodevices for water steam generation and filtration. The benefit of using wood sponges instead of previously described pure wood is the higher porosity of these structures and larger pores, which increases water uptake and flexibility (Huang et al. 2020b).

A solar steam generation device based on CNT-coated wood sponge was presented by Chen et al. (2017) (Table 2). This device had an efficiency of 81% and an evaporation rate of 11.22 kg/m^2 h at 10 suns and 65% and 0.95 kg/m^{2}h at 1 sun, respectively.

Better results were obtained by Wong et al. (2023) who coated delignified balsa wood with rGO and polypyrrole (PPY) (Table 2). The systematic experiment performed for different contents of rGO (0, 20, 40, 50, 60, 80, 100 wt%) and PPY showed that the best results were obtained for 60 wt% of rGO in PPY. The evaporation rate amounted to 1.49 kg /m^{2}h and efficiency to 93.1% at 1 Sun.

The highest evaporation rate was obtained by Li et al. (2023) who coated balsa wood aerogels with rGO (Table 2). In this study, the evaporation rate measured

under irradiance of 1 sun amounted to 2.26 kg/m^2 h and evaporation efficiency was 92.71%. The experiments performed outdoors showed that on sunny days the system was able to produce 6.39 kg/m^2 of freshwater per day. Additionally, the authors showed that the water evaporation process can generate electricity. Voltage measured along the sample after 1200 s from the start of the experiment measured at 36.2 °C amounted to 22.6 mV and a maximum current of 144 µA.

Huang et al. (2020b) used a wood sponge coated with rGO grafted with perfluorinated octyl triethoxy silane (F-rGO) to manufacture a crude oil clean-up device (Fig. 8). F-rGO coatings made the structure both superhydrophobic and oleophilic. When placed in a beaker with water and oil, the device could selectively soak only oil with a separation efficiency of 99%. The device was tested for blending oil, silicone oil, pump oil, and organic solvents—ethanol, acetone, hexane, chloroform, toluene, methanol, and DMF—and worked well for all these substances. The tests were also performed for highly viscous crude oil. It has been proposed that this substance may be effectively soaked if rGO is connected to a power source and heated electrically. Surrounding crude oil heated in such a way decreases viscosity and may be effectively cleaned up (Table 2).

Finally, it has also been demonstrated that wood-derived scaffolds and carbon nanomaterials may be useful in producing composite phase change materials (PCMs) (Table 2). Qin et al. (2021) manufactured composite PCMs using either erythritol-urea (E7U3) or erythritol-thiourea (E7T3) as base PCMs, and wood aerogels (WA) as scaffolds and CNTs as thermally conductive components. In this study, 0.5 mm thick paulownia wood samples were pretreated with a NaOH solution and soaked in DI water. Next, the samples were treated with a solution of $NaSiO_3$/NaOH/$MgSO_4$/DTPA/H_2O_2 at 80 °C, washed in DI water, and freeze-dried. Either erythritol (E) and urea (U) or erythritol (E) and thiourea (U) were mixed with CNTs. Wood aerogels were vacuum impregnated with the PCM-CNT solutions and then freeze-dried. Finally, the samples were cold pressed for 10 min at 10 MPa. It has been found that adding 1.5 wt% of CNTs into the composite was the most beneficial. The WA-E7U3-1.5CNT and WA-E7T3-1.5CNT samples kept very high latent heat values (230.3 J/g, 272.2 J/g), sufficiently low melting temperature (119.7 °C, 90.6 °C)

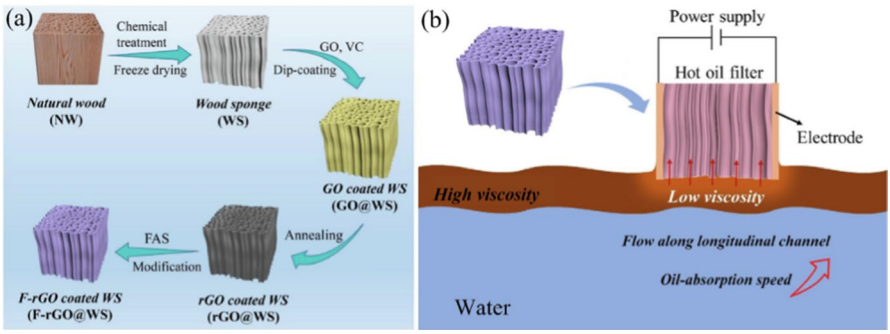

Fig. 8 **a** Manufacture of wood sponge coated with reduced graphene oxide grafted with perfluorinated octyl triethoxy silane (F-rGO). **b** Process of separating crude oil from water. Reproduced with permission from Huang et al. Huang et al. (2020b). Copyright 2020, Elsevier

and approx. 2.5 times higher thermal conductivity (0.9832 W/(m K), 0.9363 W/(m K)) than samples without CNTs. Additionally, the samples showed good chemical structure stability and excellent light-to-heat conversion performance and were characterized by good cycle stability (after 100 heating–cooling cycles). The authors also claimed that the samples were additionally electrically responsive; however, no tests were provided to demonstrate it.

Huang et al. (2022) prepared the phase change materials by compositing delignified wood with rGO, 1-tetradecanol (TD) as PCM and epoxy resin as encapsulation material. Natural balsa wood samples (10 mm × 10 mm × 10 mm) were delignified by boiling in $NaClO_2$ solution buffered with acetic acid (pH = 3.8), washed in DI water and freeze-dried. The delignified wood was infiltrated with GO water–ascorbic acid solution in a vacuum. The ascorbic-acid-assisted GO reduction process was performed by heating the samples to 150 °C for 2 h in an electric oven. Next, the samples were impregnated with melted TD. The process was carried out at 70 °C for 30 min in a vacuum chamber. After removing excess TD, two longitudinal surfaces of the samples were finished with epoxy resin by blade coating. Both the wood scaffold and the epoxy resin finish ensured very good shape stability, while keeping very high the mass fraction of TD of 88.4%. The latent heat measured by Huang et al. was comparable to the study of Qin et al. (2021) and amounted to 218.5 J/g at approx. 42 °C. Moreover, the latent heat was stable showing little change after 50 heating–cooling cycles. Finally, the electrical resistance of the samples was sufficiently low (1.85 kΩ) to demonstrate the storage of thermal energy (Joule heat) produced by the flow of electric current.

Biochars

CNMs were used to modify wood-derived biochars, increasing their adsorption properties (Table 2). Zhang et al. (2012) soaked milled cottonwood in graphene/pyrene suspension and oven-dried the mixture. The graphene-coated biochar was produced by annealing the mixture in a nitrogen atmosphere at 600 °C. The biochar was tested for the ability to adsorb polycyclic aromatic hydrocarbons (PAHs). It has been shown that the modification of cottonwood biochar with graphene increased its adsorption ability of methylene blue 20 times with regard to unmodified cottonwood biochar.

Samaraweera et al. (2021) mixed ground southern yellow pine wood chips with aqueous suspensions of three types of graphene G1 (BET surface area of 8.1 m^2/g), G2 (312 m^2/g), and G3 (712 m^2/g). The dried mixture was next pyrolyzed at 600 °C in the nitrogen atmosphere. It has been found that an increase in the BET surface area of graphenes did not contribute to better adsorption properties. The tests performed using aqueous Cu2 + suspensions showed that the best adsorption capacity was demonstrated by samples with G1, i.e., 58% more Cu2 + /m2 than raw pine biochar. This effect was attributed to the highest surface concentration of oxygenated functional groups found on G1-biochar samples.

Biochar and carbon nanomaterial in the form of graphene quantum dots were also combined to produce electrodes for supercapacitors (Zhang et al. 2020)

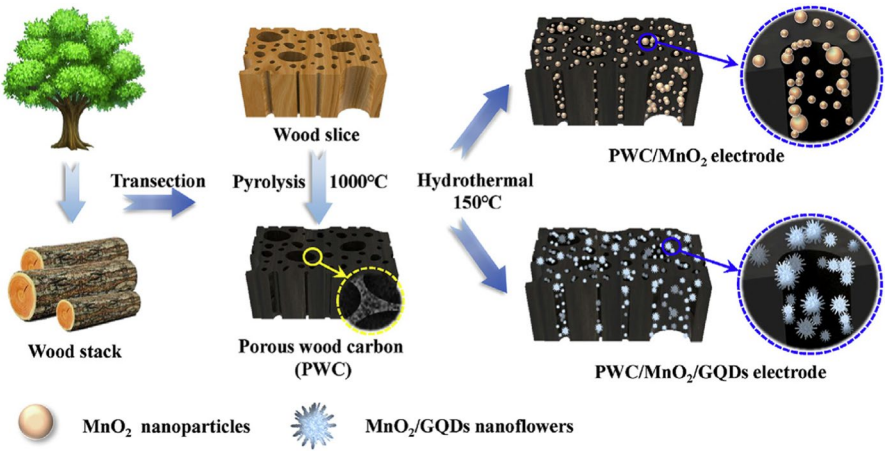

Fig. 9 Formation of supercapacitor electrodes based on biochar, MnO_2, and graphene quantum dots (GQD) composite. Reproduced with permission from Zhang et al. (2020). Copyright 2020, Elsevier

(Table 2) (Fig. 9). To produce biochar, balsa wood samples (2 cm × 2 cm × 0.1 cm) were annealed at 500 °C for 1 h and 1000 °C for 2 h in a nitrogen atmosphere. Next pseudocapacitive material MnO_2 and different contents of graphene quantum dots (GQD) were co-deposited on the biochar. The chosen amount of GQD was added to the $KMnO_4$ and Na_2SO_4 solution to obtain the coating. The solution was mixed and hydrothermally treated in an autoclave. Finally, the samples were washed with DI water and dried in a vacuum. It has been found that the best electrochemical performance was obtained for biochar coated with MnO_2 and 15 mg of GQD. This specific amount of GQD caused the growth of needle-like nanostructures at the surface of wood biochar and a significant increase in areal-specific capacitance compared to raw biochar and biochar coated with MnO_2 only. The areal-specific capacitance for PWC/MnO2/$GQDs_{15mg}$ reached 2712 mF/cm^2 at a current density of 1 mA/cm^2. The PWC/MnO2/$GQDs_{15mg}$ samples were also characterized by better rate capacitance and enhanced cycling stability (95.3% retention after 2000 cycles).

Two studies also proposed a new approach in which charred wood was used as a substrate for the chemical vapor deposition (CVD) growth of carbon nanotubes and the formation of supercapacitor electrodes (He et al. 2022; Yan et al. 2023).

He et al. (2022) carbonized balsa sheets of 5 mm thickness by heating the samples in air at 250 °C for 6 h and then for 6 h at 1000 °C in an argon atmosphere. These treatments were followed by polishing the samples which decreased their thickness to 1 mm, washing and drying. Next the samples were turned hydrophilic by immersion in 3 m KOH solution and heating at 750 °C for 2 h in argon atmosphere. After washing to neutral pH with diluted HCl, DI water and drying, the Ni catalyst was deposited on the samples by immersion in 0.25 m Ni(NO3)2 solution overnight and freeze-drying. The CVD reaction was performed by blowing Ar and H_2 mixture through as a solution of 5 g ferrocene in 100 mL xylene. The reaction was performed at 800 °C for 1 h. Next the samples were immersed in dilute HNO_3 at 60 °C overnight, then washed and freeze-dried. This procedure was expected to

remove some of the catalysts, i.e., Fe and Ni from the endings of CNTs. It has been shown that the growth of CNTs significantly increased the specific surface area of the material and density functional theory pore volume. Simultaneously, the pore width decreased which may be explained by the filling of balsa pores with CNTs. The carbonized balsa/CNT samples showed a very high areal capacitance of 1940 mF/cm^2. Interestingly, the capacitance increased by 66% after 4000 cycles which was attributed to the release of remaining Fe and Ni nanoparticles and uncovering the additional area of the inner walls of CNTs.

In the study by Yan et al. (2023), the (5 cm × 5 cm × 1 mm) basswood samples were impregnated with a solution of 0.1 g polyvinylpyrrolidone (2 mg/mL), 50 mL ethylene and 4 g of $Fe(NO_3)_3 \cdot 9\ H_2O$ by vacuum-assisted process. After air drying, the samples were placed in a vessel containing melamine and heated up in a tube furnace first up to 260 ℃ for 120 min under the N_2 flow and then up to carbonization and CVD synthesis temperatures of 700, 800, 900 and 1000 ℃ (120 min under the N_2 flow). Thus the processes of carbonization and CNT growth were performed simultaneously. Finally, the samples were immersed in 1 M HCl overnight, washed with DI water and air dried. To obtain reference samples pure balsa blocks were carbonized by the same procedure at 800 °C. The authors showed that CNT-enriched samples showed several times lower charge transfer resistance than the reference sample which additionally decreases with carbonization temperature. When used as electrodes, the samples also showed much better performance with the best results obtained for the samples carbonized at 800 °C. For this sample, the specific capacitance amounted to 6620.3 mF/cm^2, gravimetric capacitance of 118.5 F/g and volumetric capacitance of 82.8 F/cm^3 at 2 mA/cm^2. Additionally, the samples were characterized by very good cycle stability showing a capacitance retention of 94.6% after 20,000 cycles at 30 mA/cm^2. An assembled two-electrode capacitor reached a specific capacitance of 4120 mF/cm^2, a volumetric capacitance of 51.5 F/cm^3 and a gravimetric capacitance of 42.9 F/g as well as a maximum energy density of 0.6 mWh/cm^2 volumetric energy density of 6.3 mWh/cm^3 and gravimetric energy density of 6.0 Wh/kg.

Wood-based boards with carbon nanotubes

As mentioned in the introduction, wood-based boards are a subset of engineered wood products in which macroscopic or microscopic wood pieces are glued together with the smallest possible amount of adhesives. The adhesives mostly used are formaldehyde-based resins, e.g., urea–formaldehyde resin, phenol–formaldehyde resin, and melamine-urea–formaldehyde resin. For example, in MDF, the resins constitute only up to 10 wt.% of the dry wood material. Their role is to enable the formation of the solid panel and to facilitate load transfer between wood components. The aim of gluing lumber is mostly the reduction of anisotropy of mechanical properties. Similarly, the proper arrangement of veneers in plywood may also control its tensile and bending strength and stiffness in various directions. The main reason for the manufacture of fiberboards, oriented strand boards, or particleboards is the use of wood wastes and therefore decrease in the price of the panels. However, the fact

that the mechanical properties of such panels are much more uniform than in the case of pure wood is also of high importance. All the wood-based boards have to be produced in accordance with national and international standards, which set specific requirements for the density of the boards, their internal bonding strength, modulus of rupture, modulus of elasticity, thermal conductivity, water absorption, thickness swelling, emission of formaldehyde due to the presence of resins, etc. The properties of boards may be improved by applying specific coats, for example, to increase water resistance or by incorporating various substances (such as fire retardants) into the panels at the production stage. The whole panels which use wood wastes are often coated with veneers or facesheets made of other materials to improve their visual qualities, impact strength, water resistance, etc.

Incorporating CNMs into the panels could improve their properties, such as mechanical performance, thermal conductivity, or water resistance. Analogously to wood, the addition of CNMs could also enable the formation of new applications based on WBBs.

WBBs are a large group of composites. CNMs may be combined with them in several ways depending on the targeted application or specific type of board and properties to be improved. As shown by Łukawski et al. (2019a) (see "Superhydrophobic and hydrophilic coatings") any type of WBB may be coated with CNMs by dip coating, spray coating, or printing. As in the case of wood, such coatings may be hydrophobic, UV resistant, or electrically conductive (Łukawski et al. 2018, 2019a). Electrically conductive surfaces may become antistatic or serve as sensors or heaters. However, as shown in the tests of heaters (Łukawski et al. 2019a), every type of WBB has different surface roughness, which will affect the uniformity of thin coatings. Therefore in the case of specific applications, the type of WBBs and the thickness of coatings need to be adjusted.

Wood-layered composites

Chen et al. (2019) and Yan et al. (2020) showed that CNMs might also constitute a functional additive in epoxy-based coatings. In both cases, these coatings were applied on top of plywood samples to increase their fire retardancy (Table 3). Chen et al. (2019) prepared an intumescent fire retardant coating by mixing waterborne epoxy resin with melamine phosphate (MPP), melamine–formaldehyde resin (MF), pentaerythritol (PER), water, and either pure graphene oxide or graphene oxide functionalized with 3-aminopropyltriethoxysilane and H_3BO_3. The samples were prepared by brushing 3 mm thick plywood samples with the above mixtures using a wire bar coater. The reference samples were coated with pure waterborne epoxy resin and waterborne epoxy resin with MPP, MF, PER, and water. The addition of MPP, MF, and PER increased fire resistance time, intumescent factor, time to ignition, and mass of residues as well as decreased peak heat release rate, fire growth index, and average mass loss rate. However, the best improvement of these parameters was recorded when this mixture was enriched with 0.083 functionalized GO. Addition of GO and functionalized GO also increased thermal stability of the samples measured by TGA. SEM studies showed that functionalized GO-enriched char

Table 3 CNM-enriched wood-based boards developed in recent years

No	CNM	Composite	Resin	Other additives	Method of production	Properties investigated	Publication
1	GO (0.083 phr), FGO(0.042, 0.083, 0.125, 0.167 phr)	Plywood	WEP, MF	MPP, PER	Mixing, sonication, brushing with a bar coater	Flammability	Chen et al. (2019)
2	GO (0.03, 0.05, 0.07, 0.1 wt% in GPPB)	Plywood	MF	PPBs	Synthesis of GPPBs, Coating	Flammability	Yan et al. (2020)
3	COOH-MWCNTs (0.3, 0.5, and 1 wt.% In facesheets)	Plywood with epoxy or Nylon facesheet	PF	–	Mixing with facesheets, hot-pressing	Mechanical properties	Naghizadeh et al. (2017)
4	GO (0.2, 0.4, 0.6, 0.8 wt.%) reduced to rGO during hot-pressing	Pressed veneer or wood fibers	AP	Fe_2O_3	Mixing, brushing onto veneer, hot-pressing	Mechanical properties, wettability thermal stability	Chen et al. (2020b)
5	COOH-MWCNT (1.5, 3, and 5 wt.%)	MDF	UF	–	Sonication mixing with resin, hot-pressing	Thermal conductivity, mechanical properties	Gul et al. (2021)
6	GO (2, 4, or 6 wt.%)	MDF	UF	–	Sonication mixing with resin, hot-pressing	Thermal conductivity, mechanical properties	Gul et al. (2021)
7	COOH-MWCNT (0.20 and 0.52 vol%)	MDF	UF	–	Mechanical mixing with resin, cold-pressing	Mechanical properties, water intake, thermal stability	Kumar et al. (2015)
8	COOH-MWCNT (1.0, 2.5, 3.5, 5.0, 7.5, and 10.0 wt.%)	MDF	UF	–	Mechanical mixing with resin, cold-pressing	Mechanical properties, water intake	Kumar et al. (2017)
9	COOH-MWCNT (0.5, 1.0, 1.5 wt%)	MDF	UF	Al_2O_3, AC	Mechanical mixing with resin, sonication, hot-pressing	Thermal conductivity, Mechanical properties	Gupta et al. (2018)
10	MWCNT (0.4 wt%)	Fiberboard	PF	SDBS	Sonication with SDBS, Coating wood fibers, hot-pressing	Flammability, Mechanical properties	Łukawski et al (2019c)

FGO—graphene oxide functionalized with 3-aminopropyltriethoxysilane and H_3BO_3, WEP—waterborne epoxy resin, MF—melamine–formaldehyde resin, PER—pentaerythritol

MPP—melamine pyrophosphate, GPPBs—phosphate ester, AP—aluminophosphate adhesive

MDF—medium-density fiberboard, UF—urea formaldehyde resin, AC—activated charcoal

GPPBs—organophosphate-functionalized graphene oxide flame retardants

layers had better morphology and therefore were able to shield the sample more effectively.

Yan et al. (2020) synthesized flexible phosphate ester (PPB) and a set of organophosphate-functionalized graphene oxides (GPPBs) made by grafting PPB on graphene oxide. Next, the PPB and GPPBs were incorporated into amino resin and used to coat plywood samples of various dimensions. It has been shown that due to the highly exfoliated GO states, the coatings were highly transparent even at high loadings of GO. They also showed improved adhesion to the wood surface. Flammability tests (cabinet and tunnel method) showed that GO additives facilitate fire protection of the samples. The best results were obtained for GPPB3 (the lowest weight loss, char index, flame spread rating, and highest intumescent factor). Smoke density and cone calorimetry tests also showed a 60.7% reduction in smoke density rating and a 33.3% reduction in total heat release rate, respectively, for GPPB3 samples, compared to PPB samples. TGA tests also showed that GPPB3 samples showed the best thermal stability and highest residual weight. Similarly to Chen et al. (2019), the authors ascribe it to a much better char structure resulting from the presence of GO.

The publication of Łukawski et al. (2019a) also showed that CNM coatings might be incorporated into layered wood structures (see Sect. "Superhydrophobic and hydrophilic coatings"). Wood pieces were coated with raw CNTs, CNT/SDBS, and CNT/PMMA. Next, another layer of wood (decorative layer/veneer) was glued on the top using polyvinyl resin-based wood dedicated adhesive. The electrical measurements showed that on the condition that the initial CNM layer is fully black (multilayer coating), the relative change in the resistance measured before bonding and after drying of the glue is not large. The tests performed for all three types of coatings showed a change of $(9 \pm 3)\%$ for pure CNT, $(27 \pm 5)\%$ for CNT / SDBS, and $(3 \pm 4)\%$ for CNT / PMMA. This indicates that such internal layers could be successfully used as heating elements for example in flooring applications (Table 3). The only condition for proper operation of such heaters is that the decorative layer is not very thick (approx. 3 mm). Otherwise due to thermally insulating properties of wood the heat will not be transported effectively to the heated area.

Another way of incorporating CNMs into layered WBB was proposed by Naghizadeh et al. (2017), who proposed manufacturing of sandwich structured composite. Such composites typically comprise a lightweight core and two thin layers called skins/facesheets of much higher strength and stiffness than the core. Such structure imparts the sandwich composites with very high stiffness- or bending strength-to-weight ratios and excellent energy absorption properties. As wood is a common lightweight core used in such composites in many applications, Naghizadeh et al. proposed using a plywood core made of Iranian *Alnus glotinosa* veneers glued together at 90° to each other. Such an arrangement ensured that mechanical properties were more uniform and improved shear resistance. Veneers were glued using standard phenol–formaldehyde resin. As facesheets, two materials were tested: E-glass-reinforced epoxy (diglycidyl ether of bisphenol A—Epon 828, and crosslinking agent diamines of poly(oxypropylene)—Jeffamine D400), and E-glass-reinforced Nylon-6. Both polymers were used without and with the addition of COOH-functionalized MWCNTs. Eight layers of E-glass woven fabrics were cured/hot-pressed with facesheet polymers. Facesheet materials were bonded with plywood

using epoxy adhesive. It has been shown that the overall tensile properties of samples with E-glass–epoxy facesheets were much better than those with E-glass–nylon facesheets. In general, all samples improved tensile properties with the addition of CNTs. In the case of nylon samples, tensile strength, failure strain, and toughness increased with the amount of CNTs. However, in the case of E-glass epoxy facesheets, tensile strength was the highest for 0.3 wt% of CNTs. The addition of COOH-MWCNTs improved the estimated ballistic limit velocity and impact energy absorbed by both types of samples (with nylon and epoxy-based facesheets). However, the effect of reinforcement was more pronounced for nylon samples. Finally, the damaged area around the projectile point of impact was smaller in both cases, but in the case of nylon, samples were smaller than for epoxy samples (Table 3).

Particleboards

In the case of WBB, which uses smaller wood particles or fibers such as fiberboards, oriented strandboards, or particleboards, the CNMs may be incorporated more uniformly into the volume of the boards (Fig. 10). Firstly, graphene and carbon nanotubes may be mixed with resins which are further sprayed on wood components to be glued (Fig. 10a). This method would be the easiest to incorporate into any board production process, as it would not require any changes to the panels' production line. Alternatively, CNMs may also be used to modify wood particles rather than the adhesive. Wood chips/fibers may be impregnated with CNMs using methods proposed in "Synthesis of CNMs from wood" (Fig. 10b). CNMs may also be deposited on wood particles via, e.g., dip coating or spray coating (Fig. 10b). An example of wood chips dip coated in MWCNTs, and OSB board prepared using these chips is

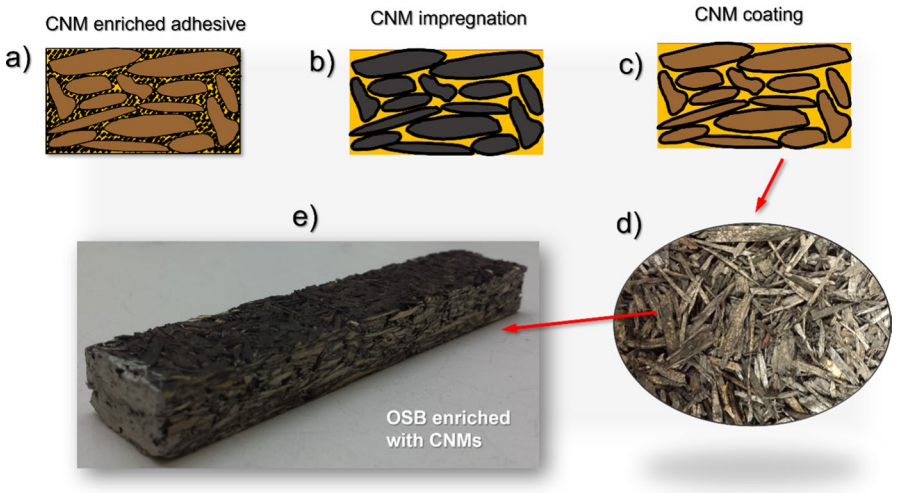

Fig. 10 Hybrid CNM-WBB produced by **a** enriching adhesive with CNMs, **b** impregnating chips/fibers with CNMs, and **c** coating chips/fibers with CNMs. **d** Image of wood chips coated with MWCNTs and **e** OSB board produced using the coated chips

presented in Fig. 10d and e, respectively. Up to now, most authors have focused on the first method of CNMs incorporation.

A very interesting work by Chen et al. (2020b) proposed that rGO may aid the fabrication of formaldehyde-free WBBs (Table 3). Currently produced WBBs use mostly formaldehyde-based resins as adhesives. Formaldehyde released from these resins may impose a severe health hazard; therefore, it has to be strictly controlled (Nielsen et al. 2017; De Cademartori et al. 2019). A solution may be using organic and inorganic formaldehyde-free adhesives (Chen et al. 2003, 2018; Liu et al. 2018; Zhang et al. 2019; Lamaming et al. 2020). However, simultaneously achieving sufficiently good mechanical performance, fire and water resistance of wood-based materials glued with these adhesives is difficult. Chen et al. (2020b) showed that mixing rGO with inorganic formaldehyde-free adhesives may enable the manufacture of plywood that fulfills Chinese National Standards for such wood-based material. The samples were prepared using poplar veneers, aluminophosphate (AP) adhesive, Fe_2O_3 as a curing agent, and graphene oxide. Veneers were glued together using adhesive mixed with rGO. Upon the formation of plywood by hot-pressing, GO is reduced to rGO. Some tests were performed for MDF prepared with the same technology and components but with poplar wood fibers instead of veneers. It has been shown that the best mechanical performance is obtained for 0.6 wt% of rGO. Dry bonding strength for such a sample amounted to 2.77 MPa compared to approx. 2.27 MPa for the reference sample. Wet bonding strength increased to 1.65 MPa (reference sample—0.8 MPa). Clearly, samples with 0.8 wt% rGO showed poorer performance than 0.6 wt% rGO, which may be attributed to the agglomeration of nanomaterials. The presence of rGO significantly increased the contact angle, from 68° to 115° for reference and 0.6 wt% GO samples, respectively. It has also been shown in TGA, limiting oxygen index, and cone calorimetry tests that the thermal stability and fire performance of rGO-enriched samples improved.

Most further studies focused on the improvement of properties of MDF boards. Gul et al. (2021) tested the properties of MDF panels enriched with COOH-functionalized MWCNTs (Table 3). All MDFs were prepared by hot-pressing poplar wood fibers coated with urea–formaldehyde resin. MWCNTs were added to test panels by sonication mixing of functionalized MWCNTs with resin. It has been found that the best properties were obtained for the samples containing 5 wt.% of functionalized MWCNTs. The samples enriched with 5 wt.% of MWCNTs improved thermal conductivity by 24.2% and reduced curing time by 20% compared to the reference sample. They also decreased formaldehyde emission by 59.4%, improved internal bonding by 21.15%, modulus of elasticity by 30.2%, modulus of rupture by 28.3%, thickness swelling by 44.8%, and water absorption by 29%.

The same authors also fabricated MDF samples enriched with graphene oxide (Gul and Alrobei 2021). Again poplar wood fibers were coated with pure or GO-enriched urea formaldehyde resin, and hot-pressed to form MDF panels. The performance of the samples improved compared to the reference samples. In most cases, the best results were obtained for 6 wt% of GO. The thermal conductivity values improved with the addition of GO by 39.79% for 6 wt% of GO reaching 0.18 W/mK. The modulus of rupture also improved by 38.8% for 6% GO. The modulus of elasticity increased by 19.22%, but the best improvement was found for 4 wt% of GO. An

increase in the concentration of GO was not beneficial to this parameter. The authors attributed this decrease to an excessively rapid resin-curing process in the presence of GO. Thickness swelling improved by 50% (6 wt% of GO) compared to the reference sample, while water absorption by 19.5% (6 wt% of GO).

Kumar et al. (2015) prepared MDF panels enriched with COOH-functionalized MWCNTs (Table 3). The samples were composed of rubber wood fibers and urea formaldehyde (UF) resin mixed with functionalized MWCNTs. Wood fibers were then coated with resins and, next, cold- and then hot-pressed to form the MDF boards. It has been shown that MWCNT-enriched resin significantly increased viscosity which is a well-known phenomenon in the case of CNTs. Further, the peak curing temperature and the resin's activation energy also decreased. The modulus of rupture of MDFs increased with the content of MWCNTs reaching the highest value for 0.52 vol% of MWCNTs. Internal bonding strength also increased with the amount of MWCNTs reaching 0.69 MPa for 0.52 vol% of MWCNTs. Formaldehyde emissions decreased with the addition of MWCNTs (7.7 mg per 100 g for 0.52 vol% of MWCNTs). Both thickness swelling and water absorption decreased with the addition of MWCNTs.

The subsequent publication of the same authors focused on using design software (Response Surface Methodology in Design Expert 7.01 software) to define the most important variables affecting MDF's manufacturing process and further its mechanical properties (Kumar et al. 2017). Modulus of rupture and internal bonding strength were chosen as the parameters to maximize. The variables included pressing time, MWCNT content, and UF resin content. The samples for experiments were prepared in the same way as in Kumar et al. (2015), but included a larger number of CNT contents. It has been found that to obtain the highest value of internal bonding of 0.75 MPa, the pressing time has to be 232 s, MWCNT content 3.5%, and UF resin content 8.18%. The best value of modulus of rupture is obtained for 238 s of pressing time, 3.1% of MWCNTs, and 7.81% of the resin. The experimental results were in good agreement with the results obtained by modeling.

Another publication of the same group compared the effect of MWCNTs functionalized with COOH, with Al_2O_3 and activated charcoal fillers (Gupta et al. 2018). The paper mainly compared results previously obtained for MWCNT-enriched MDF but also showed that adding MWCNTs may improve thermal conductivity. The highest value recorded for MWCNT loaded samples amounted to 0.153 W/mK, and an increase was higher than for other fillers.

All the above studies on MDF panels used either functionalized CNTs or GO/rGO. Such CNMs ensure very good dispersion in the adhesive, which impedes agglomeration and thus results in excellent mechanical performance. However, parameters related to water absorption may be challenging to achieve, as functionalized CNTs/GO/rGO often lose hydrophobicity. Therefore, more studies in this area may be necessary.

Only one study tested the properties of a WBB prepared via coating wood particles with CNMs and gluing coated CNMs to form a panel (Łukawski et al. 2019b) (Table 3). Scots pine (*Pinus sylvestris L.*) wood chips were dipped in an aqueous suspension of MWCNTs (0.2% w/w) and sodium dodecylbenzene sulfonate (SDBS—0.2% w/w) and then dried up to constant weight. The tests performed on

pure and coated wood chips showed a significant decrease in the decomposition rate and an increase in time to complete combustion. However, particleboards manufactured from coated chips and phenol–formaldehyde resin as adhesive did not show significant improvement in any tested properties, including flammability, water absorption, thickness swelling, and mechanical performance (modulus of rupture, elasticity, and internal bonding strength). It is possible that the weight percent of CNTs was insufficient to obtain better results, indicating that further studies in this area are necessary. Also, the role of SDBS, which was used to obtain a uniform dispersion of CNTs in water, would have to be thoroughly studied. Water in this study was used as a solvent that would be safe to use in a wood-based panels production line. However, pure CNTs are hydrophobic and cannot be suspended in water without surfactants. Therefore, it is possible that functionalized CNTs or GO/rGO would be a better choice. Alternatively, a change of surfactant or its weight percent could be investigated. Finally, it would also be interesting to investigate how an arrangement of CNMs on the wood chips rather than in the adhesive influences specific properties of the boards.

Last but not least, it would be highly desirable to prepare and test the performance of a WBB in which wood particles are impregnated with CNMs. It would be interesting to find out how much such an approach would change the mechanical, thermal, or electrical properties, water resistance, and flammability of WBBs.

Green perspectives and research gaps

Wood is a natural, sustainable, renewable and biodegradable material thus considered environmentally friendly. Indeed, thorough life cycle assessment (LSA) studies show that wood and wood products in the environmental balance sheets show definite advantages due to the low share of fossil primary energy carriers in the harvesting and processing of wood and due to the closed CO_2 cycle (Werner and Richter 2007). Wood and wood-based-products usually have favorable environmental profiles compared to other materials with the same function including steel, concrete, plastic and glass. Wood-based composites in particular have environmental benefits in terms of resource renewability and sustainability, renewable resource use efficiency, renewable biomass fuel use, lower carbon emissions (Glover et al. 2002; Pajchrowski et al. 2014; Puettmann 2022). Definitely the environmental impact of the wood harvesting, processing and manufacture of wood and wood-based products as well as their end-of-life management is not negligible. However, as shown by different studies there is still room for improvement in this respect, for example by recovery of wood waste and the use of wood in cascades (Höglmeier et al. 2014, 2015; Hossain et al. 2018; Farjana et al. 2023) or by a decrease in the energy intensity of wood drying process (Werner and Nebel 2007). It is also important to mention that many of the wood additives, coatings, adhesives, or impregnates are synthetic materials or are based on petroleum-derived products. Their use can make the materials more toxic or difficult to recycle or biodegrade. Therefore, recent studies underline that it is important to increase the use of biodegradable adhesives, paints, and impregnates (Werner and Nebel 2007; Silva et al. 2021).

Since carbon nanomaterials are still relatively new to the industry, their LCA studies are very limited (Upadhyayula et al. 2012; Arvidsson 2017; Cossutta et al. 2017; Nizam et al. 2021). Upadhyayula et al. (2012) emphasized that in the case of carbon nanotubes the most environmentally costly may be their synthesis due to the use of electrical energy for heating. This issue may need to be addressed by using energy from renewable resources. The studies on graphene highlighted that the costs differ depending on the synthesis methods and depending on the method they may be addressed by the use of greener energy sources and better recovery of chemicals used in the synthesis process (Arvidsson 2017; Cossutta et al. 2017).

Investigation of the LCA of specific CNM–wood composites is a topic for future work. However, considering general knowledge of CNMs and wood, it is already possible to draw some general conclusions. It is important to highlight that carbon nanomaterials are composed of pure carbon or are compounds of carbon, oxygen, and hydrogen. Upon combustion, which takes place at approximately 600–700 °C (Huang et al. 2014; Lepak-Kuc et al. 2018; Chen et al. 2020a), they will transform into products released upon wood combustion, such as CO or CO_2. This may indicate that, when used in pure form, carbon nanomaterials can be reused as fuel together with base wood. Recent studies on the recycling of CNT polymer composites indicate it should be possible to recycle wood-CNT composites and turn them into new composite products (Zhang et al. 2016; Chowreddy et al. 2018). Taking into account the successful transformation of wood into graphene by laser and the study of Akhavan et al. (2014) on the synthesis of GO from wood waste, we may also think about the development of other processes which would transform wood enriched with CNMs into new carbon nanomaterials (Fig. 11). These processes could be direct or use the products of combustion/pyrolysis of wood as feedstock (Xiong et al. 2005; Simate et al. 2010). Such synthesis of CNMs may also be a method of reusing wood waste. Finally, as shown by Yan et al. and Ha et al. wood waste may be upcycled into useful devices such as supercapacitor electrodes or adsorbants by co-charring and CVD synthesis of CNTs (Samaraweera et al. 2021; He et al. 2022; Yan et al. 2023).

Wood and CNMs are a perfect combination of materials for green electronics—a new field of study striving to develop human and environmentally friendly

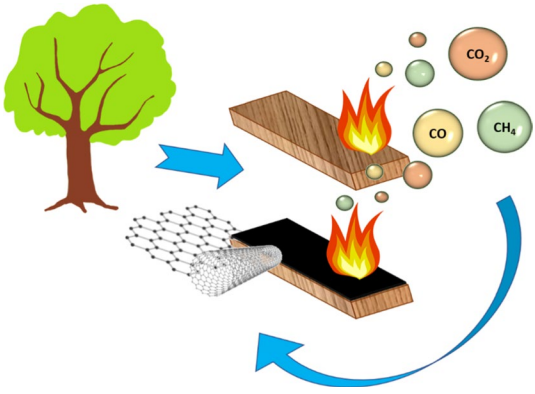

Fig. 11 Recycling of CNM-enriched wood into new carbon nanomaterials. Reprinted with permission from Lekawa-Raus (2021)

electronics. The unique electrical, thermal, chemical, and wetting properties of CNMs enable the formation of conductive or resistive electronic components and various sensors. Wood, on the other hand, is a natural, renewable, insulating support that may be the base for large-area electronic components or centimeter-scale devices. Thanks to novel processing methods, it may gain such properties as flexibility, high porosity, or extreme lightweight. In agreement with the requirements set for green electronic components (Zhu et al. 2016), wood is a highly abundant material, while CNMs may be produced on a large scale from greenhouse gasses. Electronic components manufacturing techniques such as electronic printing may also be inexpensive and high-throughput. Unlike metals or classical semiconductors used in today's electronics CNMs are all-carbon materials. Therefore, as mentioned above, it should be easier to recycle with wood supports. Up to now, the most challenging requirement may be the use of entirely non-toxic and easily biodegradable solvents, binders, and adhesives to manufacture both processed wood and CNM coatings and impregnates. This is an area for further exploration. Additional areas worth researching are the aging of green components in atmospheric conditions. Here, weathering tests (influence of humidity and UV light) and abrasion resistance tests would be highly advisable. Finally, in the case of wood sponges usage, their potential to scale up and the potential cost of mass-scale production should be considered.

The same advantages may enable the application of wood-CNM-based devices such as water steam generation, desalination systems, and filters. Their development and implementation would also be conditioned by the exploration of similar research areas. The only additional crucial aspect to be considered may be the reproducible formation of hydrophobic and hydrophilic CNM coatings (Xu et al. 2014; Stando et al. 2019).

The enhancement of wood-based boards with CNMs may lead to the development of many new products. However, until now, there is still little research regarding WBB enriched with CNMs. Most of them were focused on GO or MWCNT-OH-doped UF resin. It would be beneficial to investigate WBB using other resins, e.g., phenol–formaldehyde resin. Another important factor would be to define the influence of non-functionalized MWCNT or rGO on the mechanical, thermal, and swelling properties. Another critical question would be how the structural properties of CNMs, such as specific surface area, lateral size, thickness, length, purity, and the number of defects, relate to the properties of CNM-enhanced WBB.

In future research, it should be important to develop studies beyond the products' quality evaluation and to evaluate the environmental and economic performance of CNMs and achieve a more extensive industrial application. Furthermore, considering that currently, the processes for developing CNMs are generally at the laboratory scale, future studies should be focused on performing larger-scale trials and assessing the process's effectiveness after upscaling. Last but not least, the environmental impact of CNM-enriched wood-based materials needs to be investigated in the entire lifecycle, including the impact of CNMs manufacture, WBB production, and, finally recycling process.

Conclusion

The above review outlines major directions of studies in the newly and very rapidly emerging field of research focusing on wood and wood-based materials used in combination with carbon nanomaterials. Wood, as a natural, biodegradable, and sustainable material, is considered a very attractive base for many applications, including old ones like construction components and new ones like green electronic components or various nature-friendly nanodevices. Carbon nanomaterials in the form of pure carbon nanotubes and graphene, as well as their oxidized and functionalized forms, turn out to be very interesting additives for wood-based materials and applications. Their tunable superhydrophobic–hydrophilic properties, electrical and thermal conductivity, strength and stiffness, interesting optical properties, and chemical resistance may improve the performance of existing wood/wood-based materials and enable the formation of novel functional composites.

The review considered three groups of wood materials: wood, processed wood materials such as flexible wood aerogels (wood sponges) and biochars as well as WBBs (plywood, MDF, OSB, etc.).

The studies on wood considered first the possibility of synthesis of CNMs from wood. Wood, as a carbon-rich material, turns out to be an excellent feedstock for synthesizing graphene using fast lasers. Therefore, it would be very interesting to study other methods of synthesis of CNMs from wood-based feedstock. Such methods could enable obtaining higher yields of CNMs and decrease the cost of CNMs manufacture. Finally, the new synthesis processes would be highly interesting as a method of producing CNMs from natural and renewable resources and a new way of recycling wood waste.

Next, it has been shown that wood can be composited with CNMs by coating or impregnation. CNMs were deposited on the wood surface by various coating and printing techniques, including drop casting, spray coating, dip coating, screen printing, and laser synthesis of graphene from polymer coatings. It is important to mention that the use of binders in the formation of CNM coatings is not necessary as CNMs adhere very well to the wood surface thanks to the presence of cellulose in wood and the mechanical entrapment of CNMs on the rough surface of the wood. It has been shown that CNM coatings may be used as large-area sensors and heaters, may form hydrophobic or hydrophilic surfaces, improve the UV resistance of wood, improve thermal stability, decrease flammability, and reinforce beam support areas. It has also been demonstrated that coating wood with CNMs enabled the formation of nanodevices for solar steam generation, desalination, and filtration of heavy metals and dyes.

In most cases, impregnation of wood with CNMS was performed by dip coating and vacuum treatment. The studies showed that wood impregnation could improve mechanical properties and thermal conductivity and introduce anisotropic electrical conductivity. However, until now, only thin wood samples have been impregnated, and further studies on the methods enabling deep impregnation are necessary.

Enriching processed wood materials with CNMs may enable a wide range of new applications. Wood sponges (flexible wood aerogels) impregnated with

CNMs showed good electrical conductivity and mechanical stability while remaining highly flexible. Such materials could be used as flexible and wearable electronic components. Several authors showed that they could be applied as pressure sensors and tested them successfully as detectors of human motions. The CNM-enriched wood sponges were also applied in a gas sensing system for food quality assessment. Their shielding performance was also tested. Other applications of CNM/wood sponges composites included flexible solar steam generation devices, liquids clean-up devices (including crude oil, silicone oil, and organic solvents), and the formation of composite phase change materials.

CNMs were further used to enhance the properties of biochars. CNM additives improved the adsorption properties of biochars. The composite biochars had better adsorption ability toward polycyclic aromatic hydrocarbons and copper ions from aqueous Cu2+ suspensions. Graphene quantum dots were also composited with biochars to produce electrodes for supercapacitors.

CNMs were also tested as functional additives in various types of WBBs. The review listed various ways CNMs may be integrated with WBB, including coating, incorporation into adhesives, and coating or impregnation of wood chips. The study also considered potential properties which may be improved thanks to the incorporation of CNMs and indicated areas for further research. Until now, the studies on WBBs enriched with CNMs were not abundant. It has been shown that CNM-enriched plywood coatings could increase fire retardancy. CNM coatings and internal CNM layers were also electrically conductive and could be used as sensors, heaters, or antistatic layers. CNMs-enriched facesheets of sandwich panels were characterized by improved tensile properties, ballistic limit velocity, and impact energy absorbed. It has been demonstrated that CNMs may help fabricate formaldehyde-free wood-based boards, which would fulfill the requirements of national and international standards. MDFs glued with adhesives with CNMs were found to have better mechanical performance and thermal conductivity, lower formaldehyde emission, and lower water absorption.

The analysis of the above studies showed that all the above technologies might contribute to the development of much more environmentally and human-friendly devices, large- and small-scale electronic components, and composites. These green perspectives and the areas for further research are described in "Green perspectives and research gaps".

Acknowledgements D. Ł. would like to thank the National Center for Research and Development for co-funding the study (project no. TANGO-IV-A/0014/2019). The Table of Contents image has been designed using images (leaves and wood background) from Freepik.com.

Author contributions Literature search - D.Ł.; Literature analysis and article design - A.L.-R. and D.Ł.; Writing - original draft preparation - A.L.-R.; Writing-general information about wood - P.H.-K. and D.J.; Scientific discussion and review - D.Ł., D.J. and P.H.-K.; Data visualisation - D.Ł.; Graphics preparation (all figures aside from those where the copyright is cited) - D.Ł. and A.L.-R. All authors have read and agreed to the published version of the manuscript.

Declarations

Conflict of interest The authors have no conflict of interest to declare that are relevant to the content of this article.

References

Akhavan O, Bijanzad K, Mirsepah A (2014) Synthesis of graphene from natural and industrial carbonaceous wastes. RSC Adv 4:20441–20448. https://doi.org/10.1039/c4ra01550a

Allen MJ, Tung VC, Kaner RB (2010) Honeycomb carbon: a review of graphene. Chem Rev 110:132

Arvidsson R (2017) Review of environmental life cycle assessment studies of graphene production. Adv Mater Lett 8:187–195. https://doi.org/10.5185/amlett.2017.1413

Bauhofer W, Kovacs JZ (2009) A review and analysis of electrical percolation in carbon nanotube polymer composites. Compos Sci Technol 69:1486–1498. https://doi.org/10.1016/j.compscitech.2008.06.018

Bhatwadekar S, Conti F, Sharma K et al (2022) Co-liquefaction of sewage sludge with wheat straw in supercritical water–potential for integrating hydrothermal liquefaction with wastewater treatment plant. Sustain Energy Fuels 6:1269–2128

Boncel S, Pattinson SW, Geiser V, Shaffer MSP, Koziol KKK (2014) En route to controlled catalytic CVD synthesis of densely packed and vertically aligned nitrogen-doped carbon nanotube arrays. Beilstein J Nanotechnol 5:219

Brown E, Hao L, Gallop JC, Macfarlane JC (2005) Ballistic thermal and electrical conductance measurements on individual multiwall carbon nanotubes. Appl Phys Lett 87:023107. https://doi.org/10.1063/1.1993768

Bulyarskiy SV, Gorelik VS, Ryazanov RM (2020) Nitrogen doping of carbon nanotubes synthesized in flowing acetylene and ammonia. Inorg Mater 56:1006–1010

Cai C, Mo J, Lu Y et al (2021) Integration of a porous wood-based triboelectric nanogenerator and gas sensor for real-time wireless food-quality assessment. Nano Energy 83:105833

Chen D, He L, Shang S (2003) Study on aluminum phosphate binder and related Al_2O_3-SiC ceramic coating. Mat Sci Eng A Struct 348:29–35

Chen C, Li Y, Song J et al (2017) Highly flexible and efficient solar steam generation device. Adv Mater 29:1701756

Chen T, Wu Z, Wang X et al (2018) Hierarchical lamellar aluminophosphate materials with porosity as ecofriendly inorganic adhesive for wood-based boards. ACS Sustain Chem Eng 6:6273–6280

Chen X, Li J, Gao M et al (2019) Fire protection properties of wood in waterborne epoxy coatings containing functionalized graphene oxide. J Wood Chem Technol 39:313–328

Chen J, Lekawa-Raus A, Trevarthen J et al (2020a) Carbon nanotube films spun from a gas phase reactor for manufacturing carbon nanotube film/carbon fibre epoxy hybrid composites for electrical applications. Carbon N Y 158:282–290. https://doi.org/10.1016/j.carbon.2019.08.078

Chen T, Wu Z, Hu X et al (2020b) Constructing hydrophobic interfaces in aluminophosphate adhesives with reduced graphene oxide to improve the performance of wood-based boards. Compos Part B 198:108168

Choi W, Lahiri I, Seelaboyina R, Kang YS (2010) Synthesis of graphene and its applications: a review. Crit Rev Solid State Mater Sci 35:52

Chowreddy RR, Nord-Varhaug K, Rapp F (2018) Recycled polyethylene terephthalate/carbon nanotube composites with improved processability and performance. J Mater Sci 53:7017–7029. https://doi.org/10.1007/s10853-018-2014-0

Cossutta M, McKechnie J, Pickering SJ (2017) A comparative LCA of different graphene production routes. Green Chem 19:5874–5884. https://doi.org/10.1039/c7gc02444d

Dadile AM, Sotannde OA, Zira BD et al (2020) Evaluation of elemental and chemical compositions of some fuelwood species for energy value. Hidawi Int J for Res 2020:3457396
De Cademartori P, Artner M, De Freitas R, Magalhaes W (2019) Alumina nanoparticles as formaldehyde scavenger for urea-formaldehyde resin: rheological and in-situ cure performance. Compos B Eng 176:107281–107289
Dreyer DR, Park S, Bielawski CW, Ruoff RS (2010) The chemistry of graphene oxide. Chem Soc Rev 39:228
Ebrahimi A, Goharshadi EK, Mohammadi M (2022) Reduced graphene oxide/silver/wood as a salt-resistant photoabsorber in solar steam generation and a strong antibacterial agent. Mater Chem Phys 275:125258. https://doi.org/10.1016/j.matchemphys.2021.125258
Esmailpour A, Majidi R, Taghiyari HR et al (2020) Improving fire retardancy of beechwood by graphene. Polymers (basel) 12:303
Ewels CP, Glerup M (2005) Nitrogen doping in carbon nanotubes. J Nanosci Nanotechnol 5:1345
Farjana SH, Tokede O, Tao Z, Ashraf M (2023) Life cycle assessment of end-of-life engineered wood. Sci Total Environ 887:164018
Fernandes A, Cruz-Lopes L, Dulyanska Y et al (2022) Eco valorization of eucalyptus globulus bark and branches through liquefaction. Appl Sci 12:3775
Fu Q, Chen Y, Sorieul M (2020) Wood-based flexible electronics. ACS Nano 14:3528
Gehrke I, Geiser A, Somborn-Schulz A (2015) Innovations in nanotechnology for water treatment. Nanotechnol Sci Appl 8:1
Glover J, White DO, Langrish TAG (2002) Wood versus concrete and steel in house construction: a life cycle assessment. J for 100:34–41
Goodman SM, Bura R, Dichiara AB (2018) Facile impregnation of graphene into porous wood filters for the dynamic removal and recovery of dyes from aqueous solutions. ACS Appl Nanomater 1:5682–5690
Gspann TS, Smail FR, Windle AH (2014) Spinning of carbon nanotube fibres using the floating catalyst high temperature route: purity issues and the critical role of sulphur. Faraday Discuss 173:47–65
Guan H, Meng J, Cheng Z, Wang X (2020) Processing natural wood into a high-performance flexible pressure sensor. ACS Appl Mater Interfaces 12:46357–46365
Gul W, Alrobei H (2021) Effect of graphene oxide nanoparticles on the physical and mechanical properties of medium density fiberboard. Polymers (basel) 13:1818
Gul W, Alrobei H, Shah SR, Akbar Khan A et al (2021) Effect of Embedment of MWCNTs for enhancement of physical and mechanical performance of medium density fiberboard. Nanomaterials 11:29
Gupta A, Kumar A, Sharma KV, Gupta R (2018) Application of high conductive nanoparticles to enhance the thermal and mechanical properties of wood composite. Mater Today Proc 5:3143–3149
Gustafsson S-I (2010) The strength properties of Swedish oak and beech. Drewno 53:67–83
Han T, Nag AM, SC, Xu Y, (2019) Carbon nanotubes and its gas-sensing applications: a review. Sensors Actuators A Phys 291:107–143
Hata T, Yamane T, Kobayashi E et al (1998) Microstructural investigation of wood charcoal made by spark plasma sintering. J Wood Sci 44:332–334
Hata T, ImamuraKobayashi YE et al (2000) Onion-like graphitic particles observed in wood charcoal. J Wood Sci 46:89–92
Hazarika A, Maji TK (2014) Strain sensing behavior and dynamic mechanical properties of carbon nanotubes/nanoclay reinforced wood polymer nanocomposite. Chem Eng J 247:33–41
He Q, He R, Zia A et al (2022) Self-promoting energy storage in balsa wood-converted porous carbon coupled with carbon nanotubes. Small 18:1–10. https://doi.org/10.1002/smll.202200272
He Z, Gu Y, Liu H et al (2023) Encapsulation of wood capillary channels by electrostatically self-assembled graphene oxide for enhanced conductivity. J Porous Mater. https://doi.org/10.1007/s10934-023-01448-w
Hochmańska P, Janiszewsk D (2019) Stability and rheological behavior of nanocellulose-modified UF resin compositions. BioResources 14:1850–1866
Hochmańska-Kaniewska P, Janiszewska D, Oleszek T (2022) Enhancement of the properties of acrylic wood coatings with the use of biopolymers. Prog Org Coatings 162:106522
Höglmeier K, Weber-Blaschke G, Richter K (2014) Utilization of recovered wood in cascades versus utilization of primary wood—a comparison with life cycle assessment using system expansion. Int J Life Cycle Assess. https://doi.org/10.1007/s11367-014-0774-6
Höglmeier K, Steubing B, Weber-Blaschke G, Richter K (2015) LCA-based optimization of wood utilization under special consideration of a cascading use of wood. J Environ Manag 152:158–170

Holmberg H (2000) Influence of grain angle on Brinell hardness of Scots pine (*Pinus sylvestris* L.). Holz Als Roh Und Werkst 58:91–95

Hossain MU, Wang L, Yu IKM et al (2018) Environmental and technical feasibility study of upcycling wood waste into cement-bonded particleboard. Constr Build Mater 173:474–480

Huang X, Qi X, Boeya F, Zhang H (2012) Graphene-based composites. Chem Soc Rev 41:666

Huang L, Zhu P, Li G et al (2014) Core-shell SiO_2@RGO hybrids for epoxy composites with low percolation threshold and enhanced thermo-mechanical properties. J Mater Chem A 2:18246

Huang L, Ling L, Su J et al (2020a) Laser-engineered graphene on wood enables efficient antibacterial, anti-salt-fouling, and lipophilic-matter-rejection solar evaporation. ACS Appl Mater Interfaces 20:51864–51872

Huang W, Zhang L, Lai X et al (2020b) Highly hydrophobic F-rGO@wood sponge for efficient clean-up of viscous crude oil. Chem Eng J 386:123994

Huang W, Li H, Zheng L et al (2021) Superhydrophobic and high-performance wood-based piezoresistive pressure sensors for detecting human motions. Chem Eng J 426:130837

Huang W, Li H, Lai X et al (2022) Graphene wrapped wood-based phase change composite for efficient electro-thermal energy conversion and storage. Cellulose 29:223–232. https://doi.org/10.1007/s10570-021-04297-5

Ishii A, Kato K, Ikematsu K et al (2022) Circwood: laser printed circuit boards and sensors for affordable DIY woodworking. ACM Int Conf Proc Ser. https://doi.org/10.1145/3490149.3501317

Ishimaru K, Vystavel T, Bronsveld P et al (2001) Diamond and pore structure observed in wood charcoal. J Wood Sci 47:414–441

Ishimaru K, Hata T, Bronsveld P et al (2007) Characterization of sp2- and sp3-bonded carbon in wood charcoal. J Wood Sci 53:442–448

Janas D, Vilatela AC, Koziol KKK (2013) Performance of carbon nanotube wires in extreme conditions. Carbon N Y 62:438–446. https://doi.org/10.1016/j.carbon.2013.06.029

Janczak D, Słoma M, Wróblewski G et al (2014) Screen-printed resistive pressure sensors containing graphene nanoplatelets and carbon nanotubes. Sensors (switzerland) 14:17304–17312. https://doi.org/10.3390/s140917304

Janiszewska D, Frąckowiak I, Bielejewska N (2016) Application of selected agents for wood liquefaction and some properties of particleboards produced with the use of liquefied wood. Drewno 59:223–230

Kim D-H, Na I-Y, Jang H-K et al (2019) Anisotropic electrical and thermal characteristics of carbon nanotube-embedded wood. Cellulose 26:5719–5730

Kim Y-J, Le T-SD, Nam HK et al (2021) Wood-based flexible graphene thermistor with an ultra-high sensitivity enabled by ultraviolet femtosecond laser pulses. CIRP Ann Manuf Technol 70:443–446

Kim DH, You S, LeeJin M et al (2023) Dynamics of absorption and evaporation of organic solvents in electrically conductive wood. Cellulose 30:2413–2426. https://doi.org/10.1007/s10570-022-05018-2

Kirker G, Winandy J (2014) Chapter 6: above ground deterioration of wood and wood-based materials. In: Deterioration and protection of sustainable biomaterials. ACS symposium series American Chemical Soceity Washington, DC, pp 114–129

Kollmann FFP, Côté WA (1984) Principles of wood science and technology. I Solid Wood. Springer, Berlin

Kollmann FFP, Kuenzi EW, Stamm AJ (1975) Principles of wood science and technology. II Wood based materials. Springer, Berlin and Heidelberg GmbH & Co. KG

Koziol K, Vilatela J, Moisala A et al (2007) High-performance carbon nanotube fiber. Science 318(80):1892–1895. https://doi.org/10.1126/science.1147635

Kumar A, Gupta A, Sharma KV (2015) Thermal and mechanical properties of ureaformaldehyde (UF) resin combined with multiwalled carbon nanotubes (MWCNT) as nanofiller and fiberboards prepared by UF-MWCNT. Holzforschung 69:199–205

Kumar A, Sharma KV, Gupta A et al (2017) Optimization of processing parameters of medium density fiberboard using response surface methodology for multiwalled carbon nanotubes as a nanofiller. Eur J Wood Prod 75:203–213

Kumar A, Jyske T, Petrič M (2021) Delignified wood from understanding the hierarchically aligned cellulosic structures to creating novel functional materials: a review. Adv Sustain Syst 5:2000251

Kymalainen M, Hautamaki S, Lillqvist K et al (2017) Surface modification of solid wood by charring. J Mater Sci 52:1

La Notte L, Cataldi P, Ceseracciu L et al (2018) Fully-sprayed flexible polymer solar cells with a cellulose-graphene electrode. Mater Today Energy 7:105–112
Laine K, Segerholm K, Wålinder M et al (2016) Wood densification and thermal modification: hardness, set-recovery and micromorphology. Wood Sci Technol 50:883
Lamaming J, Heng N, Owodunni A et al (2020) Characterization of rubberwood particleboard made using carboxymethyl starch mixed with polyvinyl alcohol as adhesive. Compos B Eng 183:107731
Lamlom SH, Savidge RA (2003) A reassessment of carbon content in wood: variation within and between 41 North American species. Biomass Bioenerg 25:381–388
Lau KKS, Bico J, Teo KBK et al (2003) Superhydrophobic carbon nanotube forests. Nano Lett 3:1701–1705. https://doi.org/10.1021/nl034704t
Le T-SD, Park S, An J et al (2019) Ultrafast laser pulses enable one-step graphene patterning on woods and leaves for green electronics. Adv Funct Mater 29:1902771
Lee XJ, Hiew BYZ, Lai KC et al (2019) Review on graphene and its derivatives: Synthesis methods and potential industrial implementation. J Taiwan Inst Chem Eng 98:163–180
Lekawa-Raus A (2021) Makroskopowe przewodniki elektryczne z nanorurek węglowych. Oficyna Wydawnicza Politechniki Warszawskiej, Poland, ISBN 978-83-8156-179-2
Lekawa-Raus A, Gizewski T, Patmore J et al (2017) Electrical transport in carbon nanotube fibres. Scr Mater 131:112–118. https://doi.org/10.1016/j.scriptamat.2016.11.027
Lepak S, Warejko A, Janczak D, et al (2018) Graphene nano-flakes and carbon nanotube-based sensors via screen printing technology for acetone gases detection. In: Romaniuk RS, Linczuk M (eds) Photonics applications in astronomy, communications, industry, and high-energy physics experiments 2018. SPIE, p 37. https://doi.org/10.1117/12.2501320
Lepak-Kuc S, Boncel S, Szybowicz M et al (2018) The operational window of carbon nanotube electrical wires treated with strong acids and oxidants. Sci Rep 8:14332. https://doi.org/10.1038/s41598-018-32663-0
Li Z, Chen D, Gao H et al (2023) Reduced graphene oxide composite nanowood for solar-driven interfacial evaporation and electricity generation. Appl Therm Eng 223:119985. https://doi.org/10.1016/j.applthermaleng.2023.119985
Lin Y, Xu H, Shan X et al (2019) Solar steam generation based on the photothermal effect: from designs to applications, and beyond. J Mater Chem C 7:19203
Lisyatnikov MS, Glebova TO, Ageev SP, Ivaniuk AM (2020) Strength of wood reinforced with a polymer composite for crumpling across the fibers. IOP Conf Ser Mater Sci Eng 896:012062
Liu K-K, Jiang Q, Tadepalli SR et al (2017) Wood−graphene oxide composite for highly efficient solar steam generation and desalination. ACS Appl Mater Interfaces 9:7675–7681
Liu X, Wang K, Gu W et al (2018) Reinforcement of interfacial and bonding strength of soybean meal-based adhesive via kenaf fiber–$CaCO_3$ anchored ncyclohexyl-2-benzothiazole sulfenamide. Compos B Eng 155:204–211
Liu C, Luan P, Li Q et al (2021) Biopolymers derived from trees as sustainable multifunctional materials: a review. Adv Mater 22:2001654
Lowden LA, Hull R (2013) Flammability behavior of wood and a review of the methods for its reduction. Fire Sci Rev 2:4
Łukawski D, Lekawa-Raus A, Lisiecki F et al (2018) Towards the development of superhydrophobic carbon nanomaterial coatings on wood. Prog Org Coat 125:23–31. https://doi.org/10.1016/j.porgcoat.2018.08.025
Łukawski D, Dudkowiak A, Janczak D, Lekawa-Raus A (2019a) Preparation and applications of electrically conductive wood layered composites. Compos Part A Appl Sci Manuf 127:105656. https://doi.org/10.1016/j.compositesa.2019.105656
Łukawski D, Grześkowiak W, Dukarska D et al (2019b) The influence of surface modification of wood particles with carbon nanotubes on properties of particleboard glued with phenol-formaldehyde resin. Drewno 62:93–105. https://doi.org/10.12841/wood.1644-3985.265.03
Łukawski D, Grześkowiak W, Mazela B et al (2019c) The influence of surface modification of wood particles with carbon nanotubes on properties of particleboard glued with phenyl-formaldehyde resin. Drewno 62:93–105. https://doi.org/10.12841/wood.1644-3985.265.03
Łukawski D, Grześkowiak W, Lekawa-Raus A et al (2020) Flame retardant effect of lignin/carbon nanotubes/potassium carbonate composite coatings on cotton roving. Cellulose 27:7271–7281. https://doi.org/10.1007/s10570-020-03270-y
Łukawski D, Hochmańska-Kaniewska P, Janiszewska D et al (2022) Enriching WPCs and NFPCs with carbon nanotubes and graphene. Polymers (Basel) 14:745. https://doi.org/10.3390/polym14040745

Makgabutlane BNLN, Maubane-Nkadimeng MS, Mhlanga SD (2021) Green synthesis of carbon nanotubes to address the water-energy-food nexus: a critical review. J Environ Chem Eng 9:104736
Mehrkhah R, Goharshadi EK, Ghafurian MM, Mohammadi MMO (2021a) Clean water production by non-noble metal/reduced graphene oxide nanocomposite coated on wood: scalable interfacial solar steam generation and heavy metal sorption. Sol Energy 224:440–454
Mehrkhah R, Goharshadi EK, Mohammadi M (2021b) Highly efficient solar desalination and wastewater treatment by economical wood-based double-layer photoabsorbers. J Ind Eng Chem 101:334–347
Mohana VB, Laub K, Huic D, Bhattacharyyaa D (2018) Graphene-based materials and their composites: a review on production, applications and product limitations. Compos Part B Eng 142:200
Moosa AA, Abed MS (2021) Graphene preparation and graphite exfoliation. Turk J Chem 45:493
Murr LE, Guerrero PA (2006) Carbon nanotubes in wood soot. Atmos Sci Lett 7:93–95
Naghizadeh Z, Faezipour M, Pol MH et al (2017) High velocity impact response of carbon nanotubes-reinforced composite sandwich panels. J Sandw Struct Mater 0:1–22
Nielsen G, Larsen S, Wolkoff P (2017) Re-evaluation of the WHO (2010) formaldehyde indoor air quality guideline for cancer risk assessment. Arch Toxicol 91:35–61
Nizam NUM, Hanafiah MM, Woon KS (2021) A content review of life cycle assessment of nanomaterials: current practices, challenges, and future prospects. Nanomaterials 11:1–27. https://doi.org/10.3390/nano11123324
Norizana MN, Moklisa MH, Demona SZN, Halima NA, Samsuria A et al (2020) Carbon nanotubes: functionalisation and their application in chemical sensors. RCS Adv 10:43704–43732
Novoselov K, Fal′ko VI, Colombo L et al (2012) A roadmap for graphene. Nature 490:192
Pajchrowski G, Noskowiak A, Lewandowska A, Strykowski W (2014) Wood as a building material in the light of environmental assessment of full life cycle of four buildings. Constr Build Mater 52:428–436
Panes-Ruiz LA, Shaygan M, Fu Y, Liu Y et al (2018) Toward highly sensitive and energy efficient ammonia gas detection with modified single-walled carbon nanotubes at room temperature. ACS Sensors 3:79–86
Pei S, Cheng H-M (2012) The reduction of graphene. Carbon N Y 50:3210
Pentoś K, Łuczycka D, Wysoczański T (2017) Dielectric properties of selected wood species in Poland. Wood Res 62:727–736
Pettersen R (1984) The chemical composition of wood. In: The chemistry of solid wood. American Chemical Society, pp 57–126
Pizzi A, Papadopoulos AN, Policardi F (2020) Wood composites and their polymer binders. Polymers (basel) 12:1115
Puettmann ME (2022) Carbon analysis of wood composite panels. For Prod J 72:112–115. https://doi.org/10.13073/FPJ-D-22-00010
Qin X, Feng N, Kang Z, Hu D (2021) Construction of wood-based cellulose micro-framework composite form-stable multifunctional materials with thermal and electrical response via incorporating erythritol-urea (thiourea)-carbon nanotubes. Int J Biol Macromol 184:538–550
Richter C (2015) Wood characteristics. Description, causes, prevention, impact on use and technological adaptation. Springer, Berlin
Ross R (2021) Wood handbook—wood as an engineering material. General technical report FPL-GTR-282, Forest Products Laboratory (FPL) 2021: Madison
Rowell RM (2021) Handbook of wood chemistry and wood composites, 2nd edn. CRC Press, New York
Saito R, Dresselhaus G, Dresselhaus MS (1998) Physical Properties of Carbon Nanotubes. Imperial College Press, Anglia
Saji VS (2021) Carbon nanostructure-based superhydrophobic surfaces and coatings. Nanotechnol Rev 10:518
Samaraweera H, Pittman CU, Thirumalai RVKG et al (2021) Characterization of graphene/pine wood biochar hybrids: POTENTIAL to remove aqueous Cu2+. Environ Res 192:110283
Sandak A, Sandak J, Janiszewska D et al (2018) Prototype of the near-infrared spectroscopy expert system for particleboard identification. J Spectrosc 2018:6025163
Shishehbor P (2020) Tuning the mechanical and adhesion properties of carbon nanotubes using aligned cellulose wrap (cellulose nanotube): a molecular dynamics study. Nanomaterials 10:154
Shoukat R, Khan MI (2021) Carbon nanotubes: a review on properties, synthesis methods and applications in micro and nanotechnology. Microsyst Technol. https://doi.org/10.1007/s00542-021-05211-6

Silva VU, Nascimento MF, Resende PO et al (2021) Circular vs linear economy of building materials: a case study for particleboards made of recycled wood and biopolymer vs conventional particleboards. Constr Build Mater 285:122906
Simate GS, Iyuke SE, Ndlovu S et al (2010) The production of carbon nanotubes from carbon dioxide: challenges and opportunities. J Nat Gas Chem 19:453–460. https://doi.org/10.1016/S1003-9953(09)60099-2
Sjöström E (1993) Wood chemistry. Fundamentals and applications, 2nd edn. Academic Press, New York
Song P, Cao Z, Fu S et al (2011) Thermal degradation and flame retardancy properties of ABS/lignin: effects of lignin content and reactive compatibilization. Thermochim Acta 518:59–65
Song K, Ganguly I, Eastin I, Dichiara A (2020) High temperature and fire behavior of hydrothermally modified wood impregnated with carbon nanomaterials. J Hazard Mater 384:121283
Stando G, Łukawski D, Lisiecki F, Janas D (2019) Intrinsic hydrophilic character of carbon nanotube networks. Appl Surf Sci 463:227–233
Sun H, Ji T, Bi H et al (2021) Flexible, strong, anisotropic wood-derived conductive circuit. Adv Sustain Syst 5:2100040
Sundaram RM, Koziol KKK, Windle AH (2011) Continuous direct spinning of fibers of single-walled carbon nanotubes with metallic chirality. Adv Mater 23:5064–5068. https://doi.org/10.1002/adma.201102754
Szatkowski P, Chłopek J (2021) Biocomposites based on a balsa wood core containing intermediate layers made of coconut and sisal. Drewno 64:87–100
Tasis D, Tagmatarchis N, Bianco A, Prato M (2006) Chemistry of carbon nanotubes. Chem Rev 106:1105
Trusovas R, Ratautas K, Račiukaitis G, Niaura G (2019) Graphene layer formation in pinewood by nanosecond and picosecond laser irradiation. Appl Surf Sci 471:154–161
Upadhyayula VKK, Meyer DE, Curran MA, Gonzalez MA (2012) Life cycle assessment as a tool to enhance the environmental performance of carbon nanotube products: a review. J Clean Prod 26:37
Vanska E, Vihela T, Peresin M, Al E (2016) Residual lignin inhibits thermal degradation of cellulosic fiber sheets. Cellulose 23:199–212
Wan C, Jiao Y, Li J (2015) In situ deposition of graphene nanosheets on wood surface byone-pot hydrothermal method for enhanced UV-resistant ability. Appl Surf Sci 347:891–897
Wang L, Zhang XT, Wang XM et al (2021a) Achieving highly anisotropic three-dimensional, lightweight, and versatile conductive wood-graphene composite. Mater Today Sustain 18:100143. https://doi.org/10.21203/rs.3.rs-602232/v1
Wang Z, Han X, Zhou Z et al (2021b) Lightweight and elastic wood-derived composites for pressure sensing and electromagnetic interference shielding. Compos Sci Technol 213:108931
Werner F, Nebel B (2007) Wood and other renewable resources (subject editor: Jörg Schweinle). Int J Life Cycle Assess 12:462–463. https://doi.org/10.1065/lca2007.10.362
Werner F, Richter K (2007) Wooden building products in comparative LCA: a literature review. Int J Life Cycle Assess 12:470–479. https://doi.org/10.1065/lca2007.04.317
Wilson K, White D (1986) The anatomy of wood: its diversity and variability. Stobart Davies Ltd, New York
Wong MY, Zhu Y, Ho TC et al (2023) Polypyrrole-reduced graphene oxide coated delignified wood for highly efficient solar interfacial steam generation. Appl Thermal Eng 219:119686. https://doi.org/10.1016/j.applthermaleng.2022.119686
Wu S-S, Tao X, Xu W (2021) Thermal conductivity of poplar wood veneer impregnated with graphene/polyvinyl alcohol. Forests 12:777
Xiong GY, Suda Y, Wang DZ et al (2005) Effect of temperature, pressure, and gas ratio of methane to hydrogen on the synthesis of double-walled carbon nanotubes by chemical vapour deposition. Nanotechnology 16:532–535. https://doi.org/10.1088/0957-4484/16/4/033
Xu Z, Ao Z, Chu D et al (2014) Reversible hydrophobic to hydrophilic transition in graphene via water splitting induced by UV irradiation. Sci Rep 4:6450
Xu D, Liang G, Qi Y et al (2022) Enhancing the mechanical properties of waterborne polyurethane paint by graphene oxide for wood products. Polymers 14:5456
Xue G, Liu K, Chen Q et al (2017) Robust and low-cost flame-treated wood for high-performance solar steam generation. ACS Appl Mater Interfaces 9:15052
Yadava MD, Dasgupta K (2020) Role of sulfur source on the structure of carbon nanotube cotton synthesized by floating catalyst chemical vapour deposition. Chem Phys Lett 748:137391
Yaghoobi H, Fereidoon A (2019) Preparation and characterization of short kenaf fiber-based biocomposites reinforced with multi-walled carbon nanotubes. Compos Part B 162:314

Yan L, Xu Z, Deng N (2020) Synthesis of organophosphate-functionalized graphene oxide for enhancing the flame retardancy and smoke suppression properties of transparent fire-retardant coatings. Polym Degrad Stab 172:109064

Yan B, Feng L, Zheng J et al (2023) In situ growth of N/O-codoped carbon nanotubes in wood-derived thick carbon scaffold to boost the capacitive performance. Colloids Surf A Physicochem Eng Asp 662:131018. https://doi.org/10.1016/j.colsurfa.2023.131018

Ye R, Chyan Y, Zhang J et al (2017) Laser-induced graphene formation on wood. Adv Mater 29:1702211

Ye R, James KD, Tour JM (2018) Laser-induced graphene. Acc Chem Res 51:1609–1620

Yu Q, Jiang J, Jiang L, Al E (2021) Advances in green synthesis and applications of graphene. Nano Res 14:3724–3743

Zhang M, Gao B, Yao Y et al (2012) Synthesis, characterization, and environmental implications of graphene-coated biochar. Sci Total Environ 435–436:567–572

Zhang J, Panwar A, Bello D et al (2016) The effects of recycling on the properties of carbon nanotube-filled polypropylene composites and worker exposures. Environ Sci Nano 3:409–417. https://doi.org/10.1039/c5en00253b

Zhang B, Chang Z, Li J et al (2019) Effect of kaolin content on the performances of kaolin-hybridized soybean meal-based adhesives for wood composites. Compos B Eng 173:106919–106926

Zhang W, Yang Y, Xia R et al (2020) Graphene-quantum-dots-induced MnO_2 with needle-like nanostructure grown on carbonized wood as advanced electrode for supercapacitors. Carbon N Y 162:114

Zhang W, Wang B, Sun J et al (2022) Hive-inspired multifunctional wood-nanotechnology-derived membranes with a double-layer conductive network structure for flexible electronics. Adv Mater Interfaces 9:1–13. https://doi.org/10.1002/admi.202101727

Zhao X, Chen H, Kong F et al (2019) Fabrication, characteristics and applications of carbon materials with different morphologies and porous structures produced from wood liquefaction: a review. Chem Eng J 364:226–243

Zhu H, Luo W, Ciesielski PN et al (2016) Wood-derived materials for green electronics, biological devices, and energy applications. Chem Rev 116:9305–9374